Technische Universität München

Center for Mathematics

A Reaction-Diffusion-Advection model for bacterial quorum sensing

Peter Kumberger

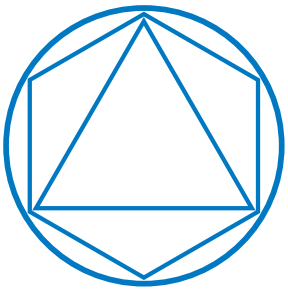

Center for Mathematics
Technische Universität München
D-85747 Garching
2013

Technische Universität München

Center for Mathematics

Master's Thesis in Mathematics

A Reaction-Diffusion-Advection model for bacterial quorum sensing

Author:	Peter Kumberger
Supervisor:	Prof. Dr. C. Kuttler
Advisor:	Dr. B. Hense
Date of Submission:	31. August 2013

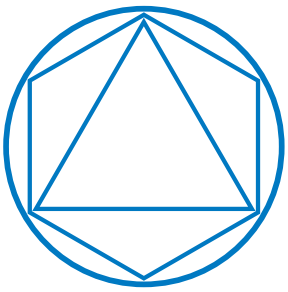

Ich erkläre hiermit, dass ich die vorliegende Masterarbeit selbstständig und nur mit den angegebenen Hilfsmitteln angefertigt habe.

München, den 31. August 2013

Abstract
Quorum sensing is a mechanism used by a broad variety of bacteria for intercellular communication. Its benefit ranges from cooperative bioluminescence to the production of virulence factors. Recently another use of quorum sensing has been postulated, namely the detachment of bacteria from a growing colony. In this thesis, we develop a model describing the colonisation, detachment and recolonisation of *Pseudomonas putida* - regulated by quorum sensing - in a flow chamber. In a first step, we neglect the spatial structure of the biological set-up. The obtained model is analysed for positivity. Afterwards, simulations are carried out to have a time course of the system and to search for bifurcations. The second part includes the before-neglected spatial structure. This model - with flow and diffusion terms taken into account - is analysed for positivity as well. Next, simplification of the model leads to the question of a possible pattern formation. In the end, the advantages of a quorum sensing regulated detachment in comparison to a constant detachment rate are considered using simulations.

Contents

1 Introduction

Bacterial quorum sensing (QS) has been studied, both experimentally and theoretically by various research groups in the last decades. It is one of many cell to cell communication mechanisms, which are found in bacteria. Quorum sensing enables the unicellular bacteria to coordinate their behaviour under certain environmental circumstances and to act as a community. It works via a signalling molecule, the so-called autoinducer (AI), which is synthesized within the cell. It is able to diffuse through the membrane of the bacterium. As long as the density of the bacteria is low, the production of autoinducers is at a low level, but when the density of the bacteria reaches a certain threshold-density, i.e., the "quorum", the positive feedback loop of the AI-production is triggered and there is a sharp increase of the production of autoinducer. Autoinducers regulate a wide variety of processes, such as bioluminescence in *Vibrio fischeri*, production of virulence factors in *Pseudomonas aeruginosa* and presumably the detachment of bacteria from the biofilm in *Pseudomonas putida*. By the switch-like change in the AI-concentration and the possibility of detecting the autoinducers, the bacteria are able to measure their own local density. This helps them to adapt their behaviour depending on the present density of bacteria. Obviously, this is an evolutionary advantage to them as some processes are only reasonable at high densities, such as the above mentioned bioluminescence and production of virulence factors.
It has been shown that quorum sensing not only depends on the local density of the bacteria, but also on the diffusible space, in which the autoinducer can accumulate, as well as other environmental factors. Therefore, quorum sensing has also been called diffusion sensing ([Red02]). In [HKM$^+$07] the two concepts of diffusion sensing and quorum sensing are brought together. Even more approaches have been published to explain the switch-like change of behaviour of bacteria at certain threshold-density ([PF10]). In this thesis, we focus on the concept of quorum sensing regulated by the local bacterial density.

In gram-negative bacteria, such as *V. fischeri* and *Pseudomonas putida*, the autoinducer is an acylated homoserine lactone (AHL). For a better understanding of quorum sensing and its positive feedback, a short desription of the quorum sensing system in *V. fischeri* is exemplarily given here. A sketch of the system is shown in figure 1.1. It has been described mathematically in [KH08].
The proteins LuxI, LuxR, AHL and complexes of AHL and LuxR are the key substances in the *lux* system of *V. fischeri*. As already mentioned above, AHL plays the role of the autoinducer and is therefore able to diffuse through the membrane of the

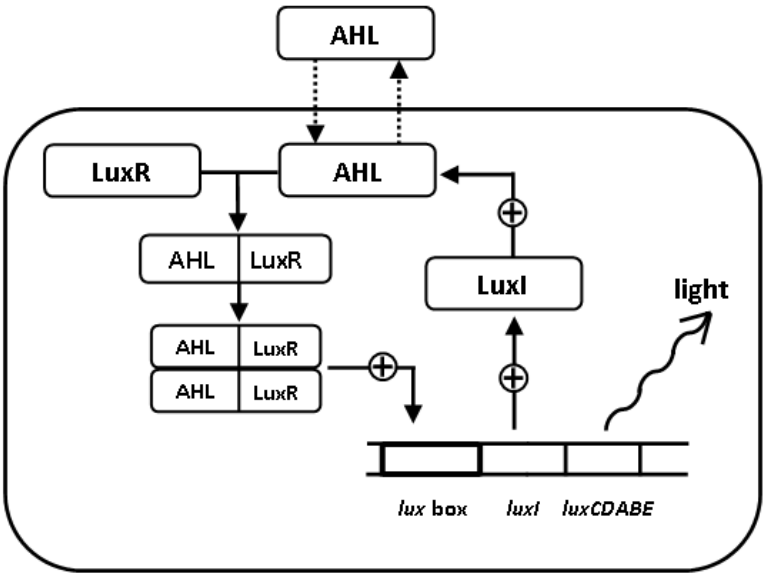

Figure 1.1: Sketch of the quorum sensing system (*lux* system) in *V. fischeri*

bacterial cells. AHL and LuxR can form monomers, which then bond to polymers. The polymers have the means for binding to the *lux* box, which in turn regulates the transcription of the *lux* genes. In this process, the components needed for the formation of luciferase, which is responsible for the bioluminescence of *V. fischeri*, are produced. Additionally, the enzyme LuxI is built during the expression of the *lux* operon. Through the direct influence of LuxI on the synthesis of AHL, cells with high concentrations of luciferase exhibit a high concentration of AHL as well.

This thesis was motivated by the results of a flow chamber experiment, as seen in [MMK+12], in which the induction of *Pseudomonas putida* under flow and non-flow conditions, using a microfluidic set-up, was investigated. Interestingly, some bacteria detached from the colonies and went into the flow. This was surprising, as leaving the colony is a disadvantage for the individual bacterium. It might be killed in the flow by antibacterial substances or might not be able to find enough nutrients. There also seemed to be a relationship between induced colonies, i.e., high concentrations of autoinducers within the bacteria of the colony, and detachment of bacteria from this colony. In this thesis, the question why the detachment of the bacteria from the colony is regulated by quorum sensing and not simply by a constant detachment rate, which would be less energy consuming, is considered. We are also interested under which conditions this regulation mechanism is beneficial for the population as a whole.
To answer those questions, we start with a spatially homogeneous model. After calculating bounds for the non-trivial stationary state, some simulations are carried out. This helps us to determine reasonable values for the unknown parameters. In

the second part, the distribution of the occuring substances (the term 'substance' will refer to proteins as well as bacteria throughout this thesis, as long as its meaning is obvious from the context) is not longer assumed spatially homogeneous. All substances are now able to diffuse and some are also influenced by the flow of the liquid in the flow chamber, in which the experiment is set up. This model is then analysed for positivity to make sure that the results are reasonable from a biological point of view and that the model used is appropriate to explain the experiment. In a next step a possible spatio-temporal pattern formation is investigated. Last, but not least, simulations are run on the earlier derived spatially inhomogeneous model, which finally enables us to answer the questions raised above.

2 Mathematical basics

2.1 Notations

At first, we introduce some notations which will be used throughout this work:

$$\partial_x := \frac{\partial}{\partial x}$$
$$\partial_t := \frac{\partial}{\partial t}$$
$$\partial_{xx} := \frac{\partial^2}{\partial x^2}$$

In section 7.1, some function spaces will be used to show the positivity of the solution of our model. Those spaces will be briefly introduced here. For more information on function spaces please refer to, e.g., [Wer11]. When investigating for a pattern formation, the space of polynomials with real coefficients is used, which is why we include it here as well.

- $d := \{(a_n)_{n\in\mathbb{N}} |\, a_n \in \mathbb{R}, a_n \neq 0 \text{ only for a finite number of } n\}$
  The space d is not a function space, but a sequence space. It is needed for the definition of the space of polynomials with real coefficients.
- $\mathbb{R}[t] := \left\{ \sum_{k=0}^{\infty} a_k x^k \,\middle|\, x \in \mathbb{R}, (a_k)_{k\in\mathbb{N}} \in d \right\}$
- $C^0(\mathbb{R}) := \{u : \mathbb{R} \to \mathbb{R} \mid u \text{ is continuous}\}$
  Norm of $C^0(\mathbb{R})$: $\|u\|_\infty := \sup_{x\in\mathbb{R}} |u(x)|$
- $C^k(\mathbb{R}) := \{u : \mathbb{R} \to \mathbb{R} \mid u \text{ is } k\text{-times continuously-differentiable}\}$
  Norm of $C^k(\mathbb{R}) := \|u\|_{C^k(\mathbb{R})} := \sum_{0\leq n\leq k} \left\|u^{(n)}\right\|_\infty$, where $u^{(n)} := \frac{d^n u}{dx^n}$
- $C^k(\mathbb{R}^n, \mathbb{R}^n) := \{u : \mathbb{R}^n \to \mathbb{R}^n |\ u \text{ is } k\text{-times continuously-differentiable}\}$
  A function $f : \mathbb{R}^n \to \mathbb{R}^n$ is called k-times continuously-differentiable, if its partial derivatives are of $C^{k-1}(\mathbb{R}^n, \mathbb{R}^n)$.
- $C^\infty(\mathbb{R}^n, \mathbb{R}^n) := \{u : \mathbb{R}^n \to \mathbb{R}^n |\ u \text{ is smooth}\}$
  A function is called smooth, if derivatives of all orders exist and are continuous.

- $L^p(\mathbb{R}) := \{u : \mathbb{R} \to \mathbb{R} \mid u \text{ is Lebesgue measurable, } \|u\|_{L^p(\mathbb{R})} < \infty\}$, where

$$\|u\|_{L^p(\mathbb{R})} := \left(\int_{\mathbb{R}} |u|^p \, dx\right)^{\frac{1}{p}}, \quad (1 \leq p < \infty)$$

  is the norm of $L^p(\mathbb{R})$.

2.2 Some introductory mathematics

Here we want to introduce some mathematical basics, which will appear throughout this thesis.

2.2.1 Bifurcations

In [Kuz04], the definition of a bifurcation reads as follows:

Definition 2.2.1. *The appearance of a topologically nonequivalent phase portrait under variation of parameters is called a bifurcation.*

In other words, a small and smooth change of the parameter values causes a sudden qualitative change in the behaviour of the system.

To explain some features of the bifurcations occuring in this thesis, the term of a stationary state and its stability shall be introduced.
Consider the initial value problem, which is defined at least for $t \in (-c, c)$ with some constant $(c \in \mathbb{R}_+)$:

$$\dot{x} = f(x); \quad x \in \mathbb{R}^n, \quad x(0) = x_0, \tag{2.1}$$

where $f \in C^\infty(\mathbb{R}^n, \mathbb{R}^n)$. The stationary state - called fixed point as well - $\bar{x}$ of the dynamical system (2.1), has the property: $f(\bar{x}) = 0$.
Therefore, there is no change of $\bar{x}$ with respect to time and hence stays constant over the course of time.
We want to define a local flow $\phi_t : \mathbb{R}^n \to \mathbb{R}^n$ by $\phi_t(x_0) = x(t, x_0)$, where $x(t, x_0)$ is a solution of problem (2.1).
The stability of the above defined fixed point describes the behaviour of the dynamical system, when $\bar{x}$ is perturbed. If the solution stays within a certain region of $\bar{x}$ for positive times, the fixed point is called Lyapunov stable (later on, we will write stable instead of Lyapunov stable). Mathematically this is formulated as follows:

$$\forall \epsilon > 0 \; \exists \; \delta > 0 : \; \|x_0 - \bar{x}_0\| < \delta \Rightarrow \|x(t, x_0) - \bar{x}(t)\| < \epsilon \; \forall t \geq 0$$

The fixed point is called unstable if and only if it is not stable.

At a bifurcation, different events depending on the type of bifurcation can be observed. One of them is the change of stability of fixed points (e.g., transcritical

bifurcation) or the change of stability of periodic orbits. Another one is the appearance or disappearance of new stationary states (e.g., saddle-node bifurcation) or the appearance of periodic orbits and a change of stability of the stationary state (e.g., Hopf bifurcation). Even more events are possible, but we want to restrict ourselves to a short description of the two bifurcations occuring in our model, namely, saddle-node and Hopf bifurcation.

In section 5.2, the term of a codimension one bifurcation will appear (for further readings on bifurcations in dynamical systems see for example [Kuz04] or [GH02]). The codimension of a bifurcation is the number of parameters, which have to be changed such that the bifurcation occurs. Thus, in our case only one parameter has to be changed. Later on, this will be the loss rate of the nutrients γ_N. In our spatially homogeneous model we have a Hopf bifurcation. Additionally, in the section of pattern formation (chapter 7.2) a saddle-node bifurcation will be mentioned.

The description of the bifurcations follows [Kuz04].
First of all, the saddle-node bifurcation shall be introduced as it is responsible for the Turing pattern formation.
Consider the following dynamical system depending on one parameter:

$$\dot{x} = f(x, \alpha), \quad x \in \mathbb{R}^n, \ \alpha \in \mathbb{R}$$

We assume that at $\alpha = 0$ this system has a nonhyperbolic equilibrium $x_0 = 0$ with the eigenvalue $\lambda_1 = 0$ and $\lambda_k < 0$ for all $k \in \{2, \dots, n\}$. Suppose that for $\alpha < 0$ there are two equilibria and for $\alpha > 0$ those have vanished. This is an example for a saddle-node bifurcation. The corresponding bifurcation diagram for a one-dimensional system with $f(x, \alpha) = \alpha + x^2$ is shown in figure 2.1. In a bifurcation diagram one can see the stationary states and its stability with respect to the bifurcation parameter. In this thesis, red lines will stand for unstable and black lines for stable stationary states.

In a next step, we take a look at the so-called Hopf bifurcation. Again consider a system

$$\dot{x} = f(x, \alpha), \quad x \in \mathbb{R}^n, \ \alpha \in \mathbb{R}$$

For simplicity assume that at $\alpha = 0$ the system has the equilibrium $x_0 = 0$ with eigenvalues $\lambda_{1,2} = \pm i\omega_0$, $\omega_0 > 0$ and $\lambda_k < 0$ for all $k \in \{3, \dots, n\}$. If λ_1 and λ_2 cross the imaginary axis as α changes from negative to positive values while the other eigenvalues stay negative, a Hopf bifurcation occurs. With the above assumptions, one can observe that while the system looses its stable stationary state on the transition of α through zero, an unstable stationary state and a stable limit cycle appear instead. For a two dimensional system this is schematically shown in figure 2.2.

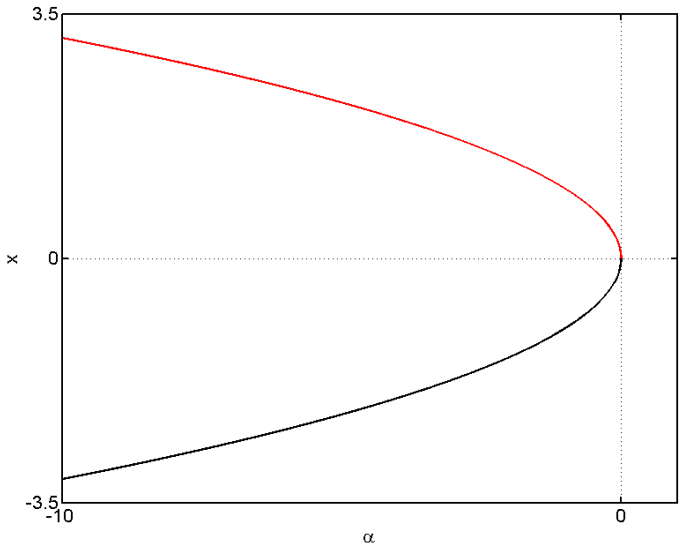

Figure 2.1: Example of a saddle-node bifurcation. The red line corresponds to unstable, the black line to stable stationary states.

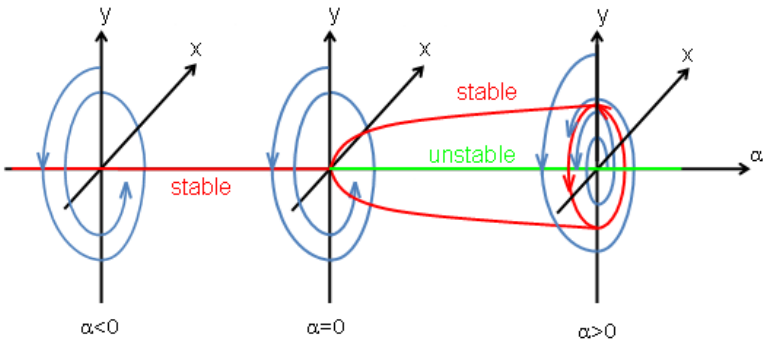

Figure 2.2: Development of a stable limit cycle due to a Hopf bifurcation (this figure is taken from [Kut09]).

2.2.2 Pattern formation

In chapter 7.2, the possibility of pattern formation is examined. Here a short idea shall be given of what such a pattern can look like.
The patterns arising from Turing and wave instabilities are both spatio-temporal patterns. While one observes a temporal homogeneous pattern, when a Turing instability is present (figure 2.3), the pattern due to a wave instability exhibits both spatial as well as temporal changes, such as travelling or standing waves (figure 2.4).
The difference between those two pattern forming mechanisms is due to two different types of bifurcations, which arise, when spatial effects are introduced into a spatially homogeneous model. While in a Turing pattern the above explained saddle-node bifurcation can be observed, a pattern due to a wave instability features a Hopf bifurcation. The bifurcation parameters in those cases are the eigenvalues of Laplace's equation.

At first, we want to show a possible figure for a Turing pattern. Therefore, in figure 2.3 the distribution over space of the variable u of the non-dimensionalised Schnakenberg system in one space dimension (model (2.2)) is shown on the top; on the bottom variable v can be seen. The Schnakenberg system has the following form:

$$\begin{aligned} \partial_t u &= \gamma(a - u + u^2 v) + \partial_{xx} u \\ \partial_t v &= \gamma(b - u^2 v) + d\partial_{xx} v \end{aligned} \qquad (x,t) \in [0,100] \times [0,100] \tag{2.2}$$

where $\gamma = 10$, $a = 0.01$, $b = 1$ and $d = 10$ were chosen for the simulation. The domain was divided into 999 equidistant cells and the figure is shown - after five million time steps - at $t_{end} = 100$, i.e., the system is already close to its stationary state. The discretisation is done in the same way as the discretisation of our PDE-model in chapter 8.1.

The example of the pattern formation due to a wave instability (figure 2.4) was taken from [DZRE00]. There, a chemical reaction described by [ZDE95] was simulated to create a figure, which is shown in figure 2.4. As we only want to give an idea of what such a pattern looks like, the model equations are left out here. For more information on the model refer to [ZDE95].

2.3 Important theorems

The last part of this section is comprised of important theorems, which will help us in the course of this work.

To formulate the first theorem, some terms have to be introduced first([GH02]):
Let us assume that $\bar{x}$ is a fixed point as described above. To study the behaviour of

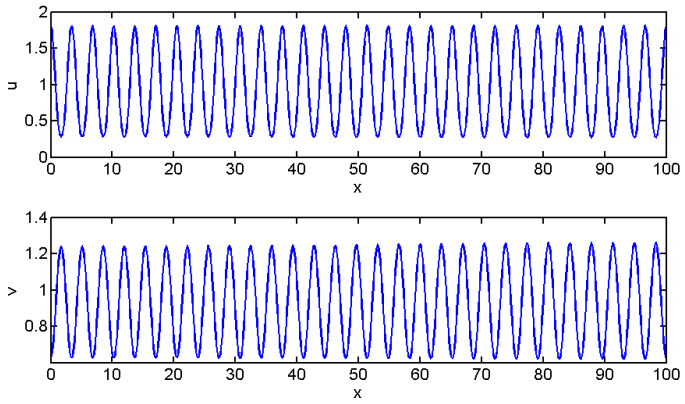

Figure 2.3: Example of a Turing pattern. The distribution over space of the variable u is shown on the top. On the bottom one can see the distribution of variable v. Both result from the non-dimensionalised Schnakenberg system at time $t = 100$.

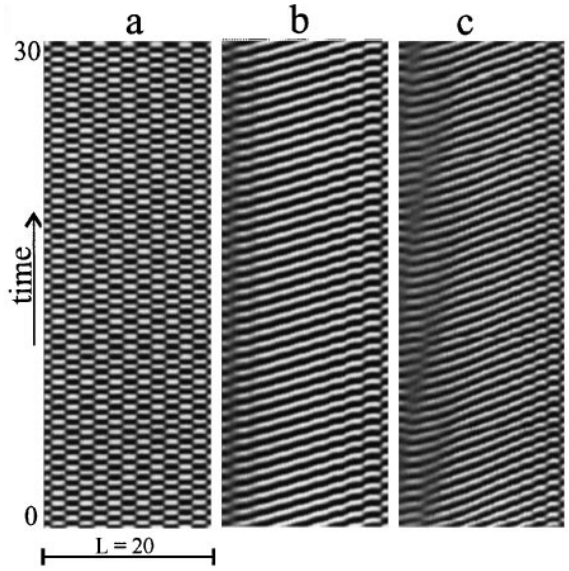

Figure 2.4: Example of different patterns due to a wave instability (figure taken from [DZRE00]) in a reaction scheme described by Zhabotinsky [ZDE95] in one space dimension. Zero flux boundary conditions and a system length of $L = 20$ were assumed. The values of one of the participating substances is shown here: white corresponds to the maximum value, black to the minimum value. (a) Standing waves; (b) Standing-traveling waves; (c) aperiodic standing-traveling waves

solutions near $\bar{x}$, the system (2.1) is linearised at $\bar{x}$:

$$\dot{\xi} = Df(\bar{x})\xi; \quad \xi \in \mathbb{R}^n, \tag{2.3}$$

where $Df = [\partial f_i/\partial x_j]$ is the Jacobian matrix of the function $f = (f_1(x_1, \ldots, x_n), f_2(x_1, \ldots, x_n), \ldots, f_n(x_1, \ldots, x_n))^T$ and $x = \bar{x} + \xi$, $|\xi| \ll 1$. Hence, the linear flow map $D\phi_t(\bar{x})\xi$ can be written as:

$$D\phi_t(\bar{x})\xi = e^{tDf(\bar{x})}\xi.$$

Now the theorem of Hartman-Grobman can be formulated. It states that the linearisation coincides with the original system in a certain neighbourhood U.

Theorem 2.3.1 (**Hartman-Grobman**). *If $Df(\bar{x})$ has no zero or purely imaginary eigenvalues then there is a homeomorphism h defined on some neighbourhood U of $\bar{x}$ in $\mathbb{R}^n$ locally taking orbits of the nonlinear flow ϕ_t of (2.1), to those of the linear flow $e^{tDf(\bar{x})}$ of (2.3). The homeomorphism preserves the sense of orbits and can also be chosen to preserve parametrisation by time.*

The next theorem is taken from [Eva10]:

Theorem 2.3.2 (**Gronwall's Lemma**). *(i) Let $\eta(\cdot)$ be a nonnegative, absolutely continuous function on $[0, T]$, which satisfies for almost every (a.e.) t the differential inequality*

$$\eta'(t) \leq \phi(t)\eta(t) + \psi(t),$$

where $\phi(t)$ and $\psi(t)$ are nonnegative, summable functions on $[0, T]$. Then

$$\eta(t) \leq e^{\int_0^t \phi(s)ds}\left(\eta(0) + \int_0^t \psi(s)ds\right)$$

for all $0 \leq t \leq T$.

(ii) In particular, if

$$\eta' \leq \phi\eta \text{ on } [0, T] \text{ and } \eta(0) = 0,$$

then

$$\eta \equiv 0 \text{ on } [0, T].$$

The Routh-Hurwitz stability criterion - as formulated below - is written down, e.g., in [Pie77]. It will be used later on to show the stability of a stationary state. To express this criterion, some terms have to be introduced first: Let $A \in \mathbb{R}^{n\times n}$. Now consider the characteristic equation, i.e., $\det(A - \lambda I) = 0$, where I is the identity matrix of $\mathbb{R}^{n\times n}$. This equation can be written as a polynomial equation:

$$\lambda^n + c_1\lambda^{n-1} + c_2\lambda^{n-2} + \ldots + c_n = 0.$$

We now define the so-called Hurwitz matrices.

Definition 2.3.1 (**Hurwitz matrix**). *The jth Hurwitz matrix, namely H_j, is defined as*

$$H_j := \begin{pmatrix} c_1 & 1 & 0 & 0 & \cdots & 0 \\ c_3 & c_2 & c_1 & 1 & \cdots & 0 \\ c_5 & c_4 & c_3 & c_2 & \cdots & 0 \\ \cdot & \cdot & \cdot & \cdot & \cdots & \cdot \\ c_{2j-1} & c_{2j-2} & c_{2j-3} & c_{2j-4} & \cdots & c_j \end{pmatrix},$$

where $c_{2p-q} = \begin{cases} c_0 = 1 & \text{if } 2p-q = 0 \\ 0 & \text{if } 2p-q < 0 \text{ or } 2p-q > n \\ c_{2p-q} & \text{else} \end{cases}$,

where p indicates the column and q the row.

With those preliminary considerations, the criterion can be stated now:

Theorem 2.3.3 (**Routh-Hurwitz stability criterion**). *All eigenvalues of A have negative real parts if and only if $\det(H_j) > 0$ for all $j = 1, \ldots, n$.*

For $n = 3$, which will be needed in section 7.2, the Hurwitz matrices are:

$$H_1 = c_1, \quad H_2 = \begin{pmatrix} c_1 & 1 \\ c_3 & c_2 \end{pmatrix}, \quad H_3 = \begin{pmatrix} c_1 & 1 & 0 \\ c_3 & c_2 & c_1 \\ 0 & 0 & c_3 \end{pmatrix}.$$

Thus, the conditions for stability are

$$\begin{aligned} (i)\, \det(H_1) &= c_1 > 0 \\ (ii)\, \det(H_2) &= c_1 c_2 - c_3 > 0 \\ (iii)\, \det(H_3) &= c_3(c_1 c_2 - c_3) > 0. \end{aligned}$$

The next theorem can be found in [Fis03] and is used in section 7.2.4.

Theorem 2.3.4 (**Complex Conjugate Root Theorem**). *If the polynomial $f \in \mathbb{R}[t]$ has a root $\lambda \in \mathbb{C}\backslash\mathbb{R}$, then the complex conjugate number $\bar{\lambda} \in \mathbb{C}$ is a root of f as well.*

The next idea concerning polynomials is taken from [HNA13].
A polynomial of third order with real coefficients, which will be used later, can be written in the following form:

$$\lambda^3 + a\lambda^2 + b\lambda + c\lambda = 0 \tag{2.4}$$

Hence, with theorem 2.3.4 a polynomial - as shown in equation (2.4) - can either have three real roots or one real root and two complex conjugated roots. In the second case those roots can be written as:

$$\lambda_{1,2} = \psi \pm i\omega, \quad \lambda_3 = \phi,$$

where $\psi, \phi \in \mathbb{R}$ and $\omega \in \mathbb{R}_+$.
Thus, the coefficients can be represented by

$$a = -(2\psi + \phi), \quad b = \psi^2 + \omega^2 + 2\psi\phi \quad \text{and} \quad c = -(\psi^2 + \omega^2)\phi.$$

Combining these equations yields

$$c - ab = 2\psi \left((\psi + \phi)^2 + \omega^2 \right).$$

When examining the model for a wave instability, we will check for a Hopf bifurcation. Thus, at the bifurcation point ψ has to be zero and therefore $c - ab \stackrel{!}{=} 0$. In section 7.2.4, the transition from a stable stationary state to a stable limit cycle is investigated, i.e., the sign of ψ has to change from negative to positive.

3 Derivation of a spatially homogeneous model

In this section, we want to derive a mathematical model for a biological setting, which we already mentioned in chapter 1 and which is outlined in figure 3.1. The variables and parameters used to describe our model, are shown in tables 3.1 and 3.2.

As it is common for mathematical modelling, some assumptions have to be made to translate the biological set-up into mathematical equations.
In the beginning, we focus on a setting where the space is assumed to be homogeneous, i.e., no consideration of spatial coordinates. Therefore, diffusion and advection processes can be neglected. In the experiment this usually happens if either the flow, diffusion or both are rather fast and the nutrients are distributed everywhere equally or the flow chamber is assumed to be rather short and thus all the substances flow through the chamber in a short period of time.
With this first assumption and the idea of a deterministic approach, i.e., assuming a high concentration of all occuring substances and bacteria and neglecting stochastic influences, we will get a five dimensional system of first order ordinary differential equations (first order ODEs) as our governing equations. Those ODEs will be nonlinear and coupled with each other. The variables will be given in concentrations or densities. The resulting concentrations and densities of our deterministic setting can be viewed as an average of the stochastic approach.
Another idea that simplifies reality, but makes the problem easier to access via mathematical tools, is to separate between bacteria which are in the biofilm and

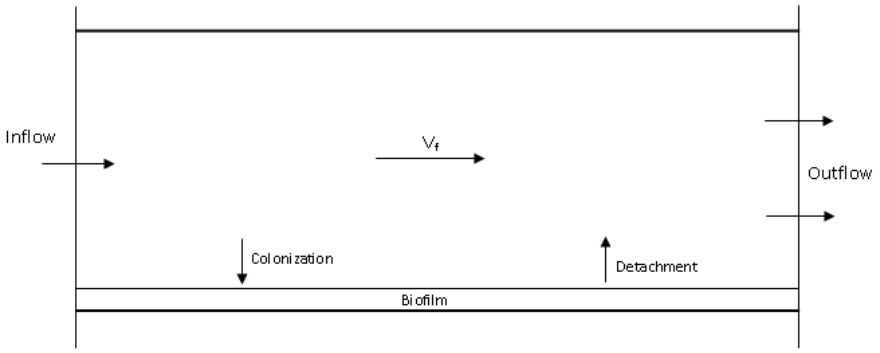

Figure 3.1: Sketch of biological set-up

bacteria which are in the flow of the flow chamber explicitely. The same will be applied to the nutrients. The biofilm is supposed to be rather thin, which leads to the assumption of a homogeneous distribution from bottom to top for all concentrations in the biofilm. Therefore, one does not have to consider the height of the flow chamber, as the exchange only happens at the boundary between the biofilm and the flow. The nutrients in the flow have to be taken into account as well. Omitting those would lead to a distribution with less nutrients downstream than upstream. As one goal of this work is to investigate the possible connection between bacteria leaving the colony and those finding a new place to settle where nutrients are abundant, a distribution of the nutrients as it is described above - not considering the nutrients in the flow - would not allow us to test our hypothesis.

The first attention is given to the derivation of the governing equation for the nutrients in the flow. A constant inflow into the flow chamber is assumed. This is realized with the constant n_0 (assuming an inhomogeneous space will lead to a different realization of the inflow). Depending on the existent concentration of nutrients, a degradation rate γ_N is added to the equation as well. A possible biological explanation for this is the abiotic degradation or the adherence of the nutrients to the walls of the flow chamber. It is also needed for the mathematical analysis (see chapter 4) later on, as it prevents an unbounded accumulation of nutrients in case there are no bacteria present. Last, but not least, a term to describe the exchange of nutrients between the flow and the biofilm is included. This term has to be multiplied by η^{-1}, because the different volumina of the biofilm and the rest of the flow chamber have to be taken into account as the variables correspond to concentrations. Thus, the parameter η corresponds to the ratio of the two volumina. We assume that bacteria in the flow do not reproduce and that AHL and nutrients have no measurable effect on B_{ext}. Therefore, the ODE for the nutrients in the flow reads as follows:

$$\dot{N}_{ext} = n_0 - \frac{c_N}{\eta}\left(N_{ext} - N_{int}\right) - \gamma_N N_{ext}$$

As well as N_{ext} the nutrients within the biofilm obviously need the same term of exchange, even though the sign has to be different. They also have the loss term

Name	Variable
B_{ext}	Density of bacteria in the flow
B_{int}	Density of bacteria in the biofilm
A	AHL-concentration in biofilm
N_{ext}	Concentration of nutrients in the flow
N_{int}	Concentration of nutrients in the biofilm

Table 3.1: Variables for model (3.4)

Name	Parameter
A_{thr1}	Threshold for AHL-induced detachment of bacteria from the colony
A_{thr2}	Induction threshold of AHL
c_1	Rate of food consumption by bacteria in the biofilm
c_A	Rate of detachment of bacteria from the biofilm
c_N	Exchange rate of nutrients between biofilm and flow
d_v	Rate of wash out of AHL by the flow
N_{thr}	Threshold for growth of bacteria in biofilm due to nutrients
n_0	Inflow of nutrients
α_A	Basal production of AHL
β_A	Stimulated AHL production
β_{int}	Growth rate of bacteria in colony due to nutrients
γ_A	Degradation rate of AHL
γ_f	Death rate of bacteria in flow
γ_N	Loss rate of nutrients
η	Fraction between thickness of biofilm and height of flow chamber

Table 3.2: Parameters for model (3.4)

γ_N, which depends on the nutrient concentration in the biofilm. The bacteria need nutrients to reproduce. In the process of reproduction, the bacteria in the biofilm consume those nutrients. The mathematical description of this process is done by using a so-called Michaelis-Menten approach (for more details please refer to [EK05] and [Mur02]). This means that if the concentration of the nutrients in the biofilm is N_{thr}, we have the half-maximal reproduction rate of the bacteria. This parameter is associated with the highest increase of the reproduction rate (see equation (3.2)). In consequence, we also get the half-maximal consumption rate of the nutrients by the bacteria at the concentration level N_{thr}. Hence, we arrive at equation (3.1) as the governing equation for N_{int}.

$$\dot{N}_{int} = c_N \left(N_{ext} - N_{int}\right) - c_1 B_{int} \frac{N_{int}}{N_{thr} + N_{int}} - \gamma_N N_{int} \tag{3.1}$$

The bacteria in the biofilm use the above mentioned reproduction term (it is just differently scaled) as well as a term which describes the detachment of the bacteria from the biofilm. It is triggered by the occurence of AHL. This term is also realized with the Michaelis-Menten approach. If the AHL-concentration is the same as A_{thr1}, one can observe the half-maximal rate of detachment of bacteria from the biofilm. We omit the possibility of death in the biofilm. Bacteria only die in the flow. If there are no nutrients available, there is no reproduction. Therefore, we find the equation for B_{int} to be:

$$\dot{B}_{int} = -c_A B_{int} \frac{A}{A_{thr1} + A} + \beta_{int} B_{int} \frac{N_{int}}{N_{thr} + N_{int}} \tag{3.2}$$

In contrast to the nutrients, AHL is considered only in the biofilm. It is assumed that by a process similar to diffusion, AHL is lost from the biofilm to the flow. Another assumption is that AHL has no effect on the bacteria in the flow (B_{ext}) as the flow transports everything quickly downstream such that AHL has no time to act on B_{ext}. Therefore AHL in the flow can be ignored. The process, in which AHL leaves the biofilm, is approximated by a constant rate d_v. There is also a degradation of AHL implemented, even though it has little effect on the dynamics of AHL as the degradation rate γ_A is small compared to d_v. More details on the choice of parameters are shown in chapter 5.1. For the production term of AHL, we assume that AHL can diffuse freely through the membrane of the cells. Mathematically we assume a compartment-barrier model (see [MMK$^+$12] for more explanation), where the biofilm is chosen to be the compartment. The production term has a basal rate α_0 and a second term, which is characteristic to positive feedback loops in a quorum sensing system on a single cell level (for more information refer to [DK01]) as it was exemplarily already explained in chapter 1. If the threshold A_{thr2} is reached, the production of AHL increases up to tenfold. Thus, the ODE for AHL has the following form:

$$\dot{A} = B_{int} \left(\alpha_A + \beta_A \frac{A^2}{A_{thr2}^2 + A^2} \right) - (\gamma_A + d_v) A$$

The only still missing governing equation describes the bacteria in the flow. The bacteria that left the biofilm are added to the bacteria in the flow. Therefore, the term for the detachment of bacteria from the biofilm through AHL is encountered here as well. It has to be multiplied by η^{-1} as in the equation for N_{ext}. In the flow the bacteria are threatened to die more often than in the biofilm because they can be eaten by other bacteria, killed by antibacterials or might not find enough nutrients. This term is important to test our hypothesis that even though it is dangerous to leave the colony (death term), it might be beneficial for the whole population to find new places to settle. Hence, the equation can be written as:

$$\dot{B}_{ext} = \frac{c_A}{\eta} B_{int} \frac{A}{A_{thr1} + A} - \gamma_f B_{ext} \tag{3.3}$$

As one can see from equation (3.3), there is no settling of bacteria from the flow into the biofilm. As our idea is that bacteria which leave the colony settle somewhere downstream at a place, where hopefully more nutrients are available, it would not be a valid choice to include such a term in the spatially homogeneous set-up. Later on, when space is considered as well, there will be a colonisation term.

So finally our model has the following form:

$$\begin{aligned}
\dot{B}_{ext} &= \frac{c_A}{\eta} B_{int} \frac{A}{A_{thr1} + A} - \gamma_f B_{ext} \\
\dot{B}_{int} &= -c_A B_{int} \frac{A}{A_{thr1} + A} + \beta_{int} B_{int} \frac{N_{int}}{N_{thr} + N_{int}} \\
\dot{A} &= B_{int} \left(\alpha_A + \beta_A \frac{A^2}{A_{thr2}^2 + A^2} \right) - (\gamma_A + d_v) A \\
\dot{N}_{ext} &= n_0 - \frac{c_N}{\eta} \left(N_{ext} - N_{int} \right) - \gamma_N N_{ext} \\
\dot{N}_{int} &= c_N \left(N_{ext} - N_{int} \right) - c_1 B_{int} \frac{N_{int}}{N_{thr} + N_{int}} - \gamma_N N_{int},
\end{aligned} \tag{3.4}$$

with suitable initial conditions

$$B_{ext}(0) = B_{ext0},\ B_{int}(0) = B_{int0},\ A(0) = A_0,\ N_{ext}(0) = N_{ext0} \ \text{ and } \ N_{int}(0) = N_{int0}.$$

4 Mathematical analysis of the ODE-model

The previously model derived will be analysed mathematically in this chapter. In a first step, the positivity of the solutions is examined. Afterwards the trivial stationary states of the system will be calculated and some bounds for the non-trivial stationary states will be formulated.
For the following calculations the parameters will be assumed non-negative. This is a reasonable assumption often used in the mathematical modelling of biological phenomena.

4.1 Positivity of the ODE-model

As our model is supposed to explain a biological set-up, we want to make sure that starting with non-negative initial conditions leads to non-negative results.
This is done by setting one variable to zero and the others are supposed to be non-negative. If the resulting derivative with respect to time of the zero-variable is non-negative, this variable will never be negative, if the other variables are non-negative.
We will check the ODE for B_{ext} exemplarily:
If $B_{ext} = 0$, $B_{int} \geq 0$ and $A \geq 0$ is applied to equation (3.3), then the resulting ODE reads as

$$\dot{B}_{ext} = \frac{c_A}{\eta} B_{int} \frac{A}{A_{thr1} + A} \geq 0$$

Thus, the density of bacteria in the flow will never change from a non-negative amount to a negative density. This is obviously important, if the model should provide biological reasonable results.
The calculations for the other ODEs are done analogously, but not shown here.

Therefore, we arrive at the desired result that our solution never returns negative values as long as the starting points are all non-negative.

4.2 Stationary states of the ODE-model

We try to find the stationary states of our spatially homogeneous model. As already explained in chapter 2 (Mathematical basics), we set all equations from model (3.4) equal to zero. For the following calculations units were omitted for better readability.

4.2.1 Trivial stationary state

Our system is in a stationary state if there are no bacteria and no AHL present and the nutrient concentration is at a saturated level, i.e., B_{ext}, B_{int} and A are zero and N_{ext} and N_{int} assume the beneath calculated values.
With the assumption of the above, one arrives at:

$$N_{int} = \frac{c_N N_{ext}}{c_N + \gamma_N}$$
$$N_{ext} = \frac{\eta n_0}{\gamma_N} \cdot \frac{c_N + \gamma_N}{c_N + \eta c_N + \eta\gamma_N}$$

As still no experimental data for the nutrients were available at the time this work was written, we decided to set the trivial stationary state of N_{ext} equal to one, i.e., we normalize N_{ext}. Thus n_0 has to be:

$$n_0 = \frac{\gamma_N(c_N + \eta c_N + \eta\gamma_N)}{\eta(c_N + \gamma_N)} \tag{4.1}$$

The numerator here will be seen more often in the following analysis. To have a more compact form, we define a new constant

$$M := \gamma_N(c_N + \eta c_N + \eta\gamma_N).$$

Taking all the above mentioned into account, leads to the following trivial stationary state of our ODE-model:

$$B_{ext} = B_{int} = A = 0$$
$$N_{ext} = 1$$
$$N_{int} = \frac{c_N}{c_N + \gamma_N}$$

4.2.2 Non-trivial stationary states

To calculate non-trivial stationary states explicitly (with no explicit values for the parameters) is not possible. With the positive feedback loop within the equation of AHL, one has to solve a polynomial of third order to get an analytical solution for the stationary state of AHL. Even the usage of a mathematical tool like MAPLE will not give reasonable results.
But one can formulate some conditions for the stationary states. By solving the governing equation of N_{ext}, we get:

$$N_{ext} = \frac{\eta n_0 + c_N N_{int}}{c_N + \eta\gamma_N} \tag{4.2}$$

Inserting this result into the governing equation of N_{int}, leads after some calculations to a rather complicated solution for the stationary state of N_{int}:

$$N_{int} = \frac{-f(B_{int}) \pm \sqrt{(f(B_{int}))^2 + 4M\eta n_0 c_N N_{thr}}}{2M}$$

where $f(B_{int})$ is:

$$f(B_{int}) = MN_{thr} + c_1 B_{int}(c_N + \eta\gamma_N) - \eta n_0 c_N$$

If $f(B_{int})$ is assumed to be bigger than zero, i.e.,

$$B_{int} \geq \frac{n_0\eta}{c_1} \cdot \frac{c_N - c_N N_{thr} - \gamma_N N_{thr}}{c_N + \eta\gamma_N}, \tag{4.3}$$

whereat the definition for n_0 from equation (4.1) was used, some conditions can be formulated.
Using $a^2+b^2 \leq (a+b)^2$ for $a, b \geq 0$, leads to the following condition for the stationary state of N_{int}:

$$N_{int} \leq \sqrt{\frac{c_N N_{thr}}{c_N + \gamma_N}}$$

The so obtained condition for N_{int} inserted into equation (4.2) results in the following inequality:

$$N_{ext} \leq \frac{M + c_N\sqrt{c_N N_{thr}(c_N + \gamma_N)}}{(c_N + \gamma_N)(c_N + \eta\gamma_N)}$$

Now we get an upper bound for the stationary state of B_{ext} as well:

$$B_{ext} \geq \frac{\beta_{int} M}{\eta\gamma_f c_1} \cdot \frac{c_N - \sqrt{c_N N_{thr}(c_N + \gamma_N)}}{(c_N + \eta\gamma_N)(c_N + \gamma_N)}$$

So we formulated bounds for the stationary states. In case B_{int} satisfies the above mentioned condition (4.3), the stationary states for N_{ext} and N_{int} have to be smaller and B_{ext} has to be greater than the calculated values.
As already indicated earlier, it is hard to calculate any reasonable solution for AHL. Therefore, we were not able to limit A to a range of values as it was possible with the other variables.

4.3 Summary of the achieved results

In this chapter, we were able to show the positivity of our solutions in the spatially homogeneous model. As it was already mentioned, this is a necessary condition for a model describing our biological experiment as negative concentrations would not be reasonable.

We also calculated the trivial stationary state, in which no bacteria and no AHL are present and the nutrient concentration is at a saturated level. While it was not possible to calculate the non-trivial stationary state analytically, we were able to specify limits, within which the values for the stationary state have to lie.

5 Simulations on the ODE-model

In this chapter, the previously derived and analytically examined ODE-model is simulated. In a first step, we assign values to the occuring parameters such that the simulations can be executed. Then we simulate the model to see if it exhibits bifurcations.
The following simulations were done with Matlab ([Mat10]) as well as XPPAUT ([Erm03]).

5.1 Choice of parameters

To simulate our model, values for the parameters are needed. While some of them were obtained from literature, others were chosen through the careful use of simulations to show the expected typical behaviour.
The values for A_{thr2}, α_A, β_A, β_{int} and γ_A were taken from [MMK+12].

Parameter	Value	Parameter	Value
A_{thr1}	$2.1\,\frac{nmol}{ml}$	A_{thr2}	$0.07\,\frac{nmol}{ml}$
c_1	$5 \cdot 10^{-10}\,\frac{nmol}{Bact \cdot h}$	c_A	$0.693\,\frac{1}{h}$
c_N	$35\,\frac{1}{h}$	d_v	$554.5\,\frac{1}{h}$
N_{thr}	$0.5\,\frac{nmol}{ml}$	n_0	$1.03\,\frac{1}{h}$
α_A	$2.3 \cdot 10^{-10}\,\frac{nmol}{Bact \cdot h}$	β_A	$2.3 \cdot 10^{-9}\,\frac{nmol}{Bact \cdot h}$
β_{int}	$0.4\,\frac{1}{h}$	γ_A	$0.005545\,\frac{1}{h}$
γ_f	$1000\,\frac{1}{h}$	γ_N	$1\,\frac{1}{h}$
η	30		

Table 5.1: Values of parameters for simulations

The detachment threshold A_{thr1} is chosen such that the bacteria can reach a reasonable density within the biofilm. The exact value originates from the simulations.
The fraction between the thickness of the biofilm and the height of the flow chamber η is assumed to be 30. In our case this is deduced from the assumption that a biofilm is about $13\mu m$ high.
The strength of detachment c_A is defined such that 50 percent of the bacteria in the biofilm have already detached themselves after one hour.

AHL is washed out due to the flow with the rate d_v. In order to observe biological reasonable densities of the bacteria in the biofilm, the rate of wash out has to be big compared to γ_A or otherwise the bacteria detach already at low AHL-concentrations. So far little is known about the interplay of nutrients and quorum sensing. Therefore, for most parameters concerning the nutrients values are unknown. We chose them such that the simulations showed a biological relevant behaviour. As no experimental data is available, the nutrients are assumed to be dimensionless. The threshold concentration of nutrients in the biofilm N_{thr}, at which the reproduction rate is the highest, was chosen to be half of the capacity of nutrients in the flow.
Nutrients are exchanged between the biofilm and the flow with the exchange rate c_N. It is chosen in such a fashion that the nutrients are in an equilibrium after about twelve minutes. This is a rather fast process, but it is needed such that the bacteria have enough food provided to grow up to reasonable big colonies.
The amount of nutrients a bacterium needs to reproduce is assumed high; hence, the effect of starvation in a fully colonised biofilm can be observed. An idea - examined in a later chapter - is the advantage for the whole population of bacteria's detachment from the biofilm, when the nutrients are limited, and recolonising new sites.
The parameters γ_N and n_0 were changed in the process of creating the bifurcation diagram. If not mentioned otherwise, they assume the values shown in table 5.1. The value of n_0 depends on the values of γ_N, η and c_N (refer to equation (4.1) in chapter 4.2.1). The degradation rates of the nutrients in the flow as well as in the biofilm are assumed to be small such that not too many nutrients are lost due to degradation.

5.2 Results of the simulations

As initial conditions for the simulations of our ODE-model we assume that there are no bacteria in the flow and no AHL in the biofilm. The whole flow chamber is supposed to be saturated with nutrients, i.e., $N_{ext} = N_{int} = 1$, and one bacterium is located in the biofilm-layer, i.e. $B_{int} = 1.2 \cdot 10^{10} Bact/ml$ at the beginning of the simulation. The bacterial density in the biofilm is calculated by

$$B_{int} = \frac{\text{Number of bacteria}}{\text{Volume of biofilm}}.$$

The volume of biofilm is calculated by the height ($h = 13\mu m$) and the area occupied by one bacterium. This area is about $6\mu m$ as it is assumed that only around 16% of the biofilm are occupied by bacteria. The remaining volume is comprised of extracellular polymeric substances ([CLC+95]).

Figure 5.1 shows the time course of our homogeneous system with the above mentioned initial conditions and the parameter values from table 5.1. While in the top

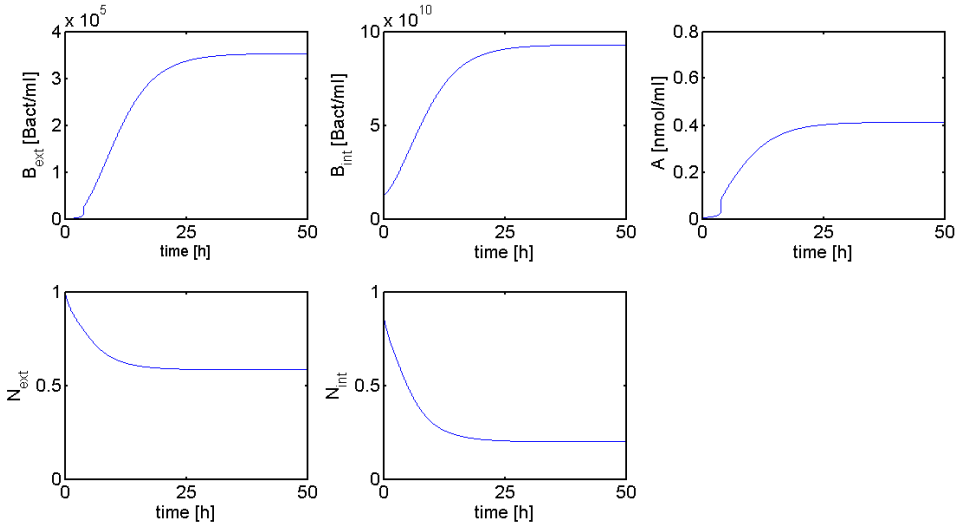

Figure 5.1: Time course of the ODE-model

left corner of this figure one can see, how the density of the bacteria in the flow behave over time, the time course of the bacterial density in the biofilm is shown in the middle of the upper row. Next to it the AHL-concentration is displayed. In the lower row, the time course of the nutrient concentration in the flow is presented on the left and the time course of the nutrient concentration in the biofilm on the right. One can observe that already after about four hours the so-called "quorum" of the bacteria in the biofilm is reached and a strong increase of the AHL-production can be noticed. This results in a fast accumulation of AHL. This happens, when there are between two and three bacteria in the biofilm, which is a surprisingly small number. At this time, one can also see a sharp increase of the bacterial density in the flow due to the detachment of bacteria from the biofilm, which is regulated by the AHL-concentration. About 25 hours after the start of the simulation a stationary state is approximately reached, in which all the traced quantities stay constant. The bacteria in the biofilm are switched on and move to the flow with a constant rate. There are still nutrients in the flow chamber available, so the bacteria in the biofilm are able to reproduce. The colony consists of around eight bacteria in the stationary phase.

The model, which was developed to describe our biological set-up, has the mathematically interesting feature of a codimension 1 bifurcation, namely a Hopf bifurcation. In chapter 2, we already introduced the idea of this kind of bifurcation. The corresponding bifurcation diagram is shown in figure 5.2. The loss rate of the nutrients γ_N was used as a bifurcation parameter. But as already mentioned above, the inflow of nutrients n_0 also depends on γ_N and hence is changed as well. Figure 5.2(b) gives details for figure 5.2(a) as the Hopf bifurcation taking place for small γ_N cannot be seen otherwise. From these two figures it is obvious that there are

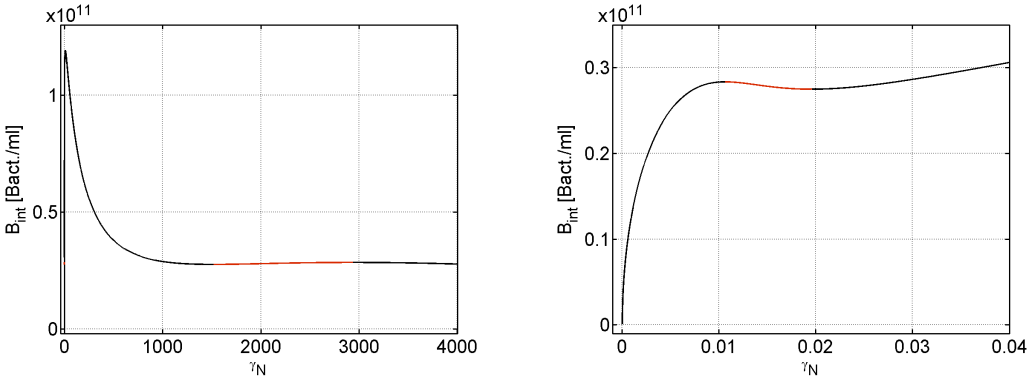

(a) (b)

Figure 5.2: (a) Bifurcation diagram of the homogeneous model for the loss parameter γ_N. (b) Details of figure 5.2(a) for small γ_N.

two Hopf bifurcations - one for small and one for high loss rates. While the black lines correspond to stable stationary states, the red lines correspond to unstable stationary states. As it is characteristic to Hopf bifurcations, stable limit cycles can be observed for the range of γ_N, where unstable stationary states occur.
To get a better understanding of the time course of a stable periodic orbit in our model, figure 5.3 is included. The initial conditions are the same as in figure 5.1. Interestingly, the two limit cycles - as seen in figure 5.3 - have the same appearance for the bacterial and the AHL-concentration even though the loss rate - and therefore the inflow - of the nutrients differs significantly. While for small γ_N a fast approach to the limit cycle can be observed, the approach is considerably slower, when we assume a high loss rate. This is mathematically interesting, but the change of B_{int} lays within the density of one bacterium and is therefore biologically not relevant. However, it should be investigated more carefully, when a non-deterministic approach is considered as a periodically changing biofilm thickness has been observed already *in vitro* ([ZKR+99]) and it is most likely to be encountered in this biological set-up under certain environmental circumstances as well.

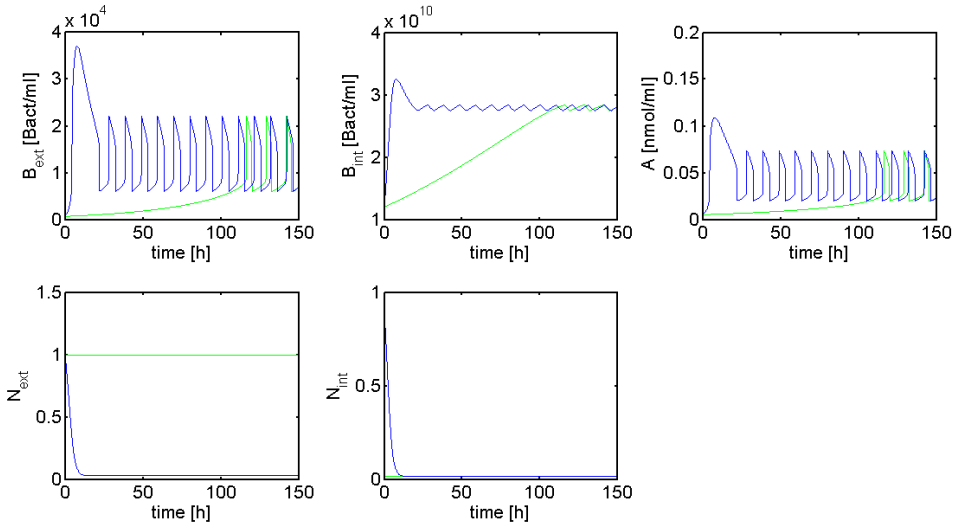

Figure 5.3: Time course of the ODE-model with the death rate of the bacteria in the flow chosen such that oscillations can be observed. Blue line: $\gamma_N = 0.015$. Green line: $\gamma_N = 2400$.

6 Derivation of a spatially inhomogeneous model

So far, we neglected the spatial structure of the biological set-up. In this section, we want to expand model (3.4) such that it is able to explain the behaviour of our bacteria in space as well as in time. This will lead to a semi-linear parabolic system of partial differential equations (PDEs). Some new parameters will be introduced to allow an explanation of the newly introduced extensions of the model. They can be seen in table 6.1.

As our model is supposed to describe an experimental set-up in a flow chamber, spatial influences should be incorporated into the model, i.e., the occuring substances and bacteria depend on a time variable as well as on a space variable. In order to keep the model convenient to work with, we assume the behaviour of our system to be homogeneous perpendicular to the flow direction, meaning that we can neglect one space-dimension. In the following, the space-dimension in the direction of the flow will be called x-direction. We still distinguish between substances in the biofilm and in the flow as already seen in chapter 3.

The most obvious extension is to let the occuring substances and bacteria diffuse at specified rates. To realise this idea, we add to each governing equation the corresponding diffusion term ($\frac{\partial^2}{\partial x^2}$).

In a next step, a term to describe the process of colonisation of the biofilm by the bacteria of the flow is included in the governing equations of B_{ext} and B_{int}. The bacteria from the flow are only supposed to colonise the biofilm if no bacteria in the biofilm are present in the distance δ_b upstream. So the PDE for the bacteria in the biofilm changes to be

$$\frac{\partial B_{int}}{\partial t} = D_{B_{int}} \frac{\partial^2 B_{int}}{\partial x^2} + c_b e^{-\int_{h_1(x)}^{x} cB_{int}(t,s)ds} B_{ext} - c_A B_{int} \frac{A}{A_{thr1} + A} + \beta_{int} B_{int} \frac{N_{int}}{N_{thr} + N_{int}}, \tag{6.1}$$

where $h_1(x) := \begin{cases} x - \delta_b & \text{if } x - \delta_b > 0 \\ 0 & \text{else} \end{cases}$.

Name	Parameter
c	Strength of the avoidance of recolonisation due to other bacteria in the biofilm
c_b	Colonisation rate of the biofilm by the bacteria in the flow
δ_b	Region upstream, which the bacteria examine in order to colonise the biofilm if it is empty
$D_{B_{ext}}$	Diffusion coefficient of bacteria in the flow
$D_{B_{int}}$	Diffusion coefficient of bacteria in the biofilm
D_A	Diffusion coefficient of AHL
$D_{N_{ext}}$	Diffusion coefficient of nutrients in the flow
$D_{N_{int}}$	Diffusion coefficient of nutrients in the biofilm
n_{inflow}	Concentration of nutrients in the flow at the left boundary
v_f	Velocity of flow

Table 6.1: Definition of the newly introduced parameters (parameters of the ODE-model are shown in table 3.2)

The form of this colonisation term is justified by the assumption that, if there are any bacteria close - in the upstream direction - there should be no colonisation. This idea is realised by the sharp drop of the exponential function.

Additionally, the influence of the flow has to be taken into account in the spatially inhomogeneous model. Our idea to introduce this effect is to neglect any flow in the biofilm and hence only consider flow in the PDEs of B_{ext} and N_{ext}. Thus, the resulting governing equation for B_{ext} reads as follows

$$\frac{\partial B_{ext}}{\partial t} = D_{B_{ext}} \frac{\partial^2 B_{ext}}{\partial x^2} - v_f \frac{\partial B_{ext}}{\partial x} - \frac{c_b}{\eta} e^{-\int_{h_1(x)}^{x} cB_{int}(t,s)ds} B_{ext} + \frac{c_A}{\eta} B_{int} \frac{A}{A_{thr1} + A} - \gamma_f B_{ext}. \tag{6.2}$$

The governing equations for AHL and the nutrients in the biofilm stay the same as seen in chapter 3, except for the diffusion-terms. In the PDE describing the dynamics of N_{ext}, the inflow of nutrients is realised differently to the ODE-model (3.4). Instead of explicitly appearing in the governing equation the inflow is now part of the boundary condition. It is realised by an inhomogeneous Dirichlet boundary condition. Thus, the concentration of the nutrients at the left boundary assumes the value n_{inflow}.

Unless stated otherwise, the PDEs are considered on $(t_0, t_{end}) \times [0, x_{end})$.

According to the above introduced changes, i.e., assuming the distribution of the substances in the flow-direction to be inhomogeneous, the complete model has the following form

$$
\begin{aligned}
\frac{\partial B_{ext}}{\partial t} =& D_{B_{ext}} \frac{\partial^2 B_{ext}}{\partial x^2} - v_f \frac{\partial B_{ext}}{\partial x} - \frac{c_b}{\eta} e^{-\int_{h_1(x)}^{x} cB_{int}(t,s)ds} B_{ext} + \frac{c_A}{\eta} B_{int} \frac{A}{A_{thr1} + A} - \gamma_f B_{ext} \\
\frac{\partial B_{int}}{\partial t} =& D_{B_{int}} \frac{\partial^2 B_{int}}{\partial x^2} + c_b e^{-\int_{h_1(x)}^{x} cB_{int}(t,s)ds} B_{ext} - c_A B_{int} \frac{A}{A_{thr1} + A} + \beta_{int} B_{int} \frac{N_{int}}{N_{thr} + N_{int}} \\
\frac{\partial A}{\partial t} =& D_A \frac{\partial^2 A}{\partial x^2} + B_{int} \left(\alpha_A + \beta_A \frac{A^2}{A_{thr2}^2 + A^2} \right) - (\gamma_A + d_v) A \\
\frac{\partial N_{ext}}{\partial t} =& D_{N_{ext}} \frac{\partial^2 N_{ext}}{\partial x^2} - v_f \frac{\partial N_{ext}}{\partial x} - \frac{c_N}{\eta} \left(N_{ext} - N_{int} \right) - \gamma_N N_{ext} \\
\frac{\partial N_{int}}{\partial t} =& D_{N_{int}} \frac{\partial^2 N_{int}}{\partial x^2} + c_N \left(N_{ext} - N_{int} \right) - c_1 B_{int} \frac{N_{int}}{N_{thr} + N_{int}} - \gamma_N N_{int},
\end{aligned}
\tag{6.3}
$$

with homogeneous Neumann boundary conditions for all variables, but N_{ext}, on the left boundary and an inhomogeneous Dirichlet boundary condition for N_{ext}

$$
\begin{aligned}
\frac{\partial B_{ext}(t,0)}{\partial x} = \frac{\partial B_{int}(t,0)}{\partial x} = \frac{\partial A(t,0)}{\partial x} = \frac{\partial N_{int}(t,0)}{\partial x} = 0 \\
N_{ext}(t,0) = n_{inflow},
\end{aligned}
\tag{6.4}
$$

and initial conditions

$$
\begin{aligned}
B_{ext}(0,x) = B_{ext0}(x),\ B_{int}(0,x) = B_{int0}(x),\ A(0,x) = A_0(x) \\
N_{ext}(0,x) = N_{ext0}(x),\ N_{int}(0,x) = N_{int0}(x).
\end{aligned}
\tag{6.5}
$$

7 Mathematical analysis of the PDE-model

At first, we will analyse model (6.3) - (6.5) for positivity of its solutions. Then the model is examined for a potential pattern formation. For this purpose the model will be simplified assuming different time scales. Afterwards, the stationary states of the so-derived model will be calculated, assuming a spatially homogeneous distribution of the substances again. Finally some conclusions about pattern formation are drawn.

7.1 Positivity of solutions

In biological problems treated with mathematical tools, a question that often has to be answered, is the positivity of solutions. As negative quantities in biology most of the time make no sense, the solutions of the governing equations in the mathematical model should be non-negative for all times, in which a solution exists. The existence and uniqueness of solutions of model (6.3) with inital conditions (6.5) and the boundary condition (6.4) up to time t_{end} are not subject to this work and will be unconditionally assumed for the following parts. For more information on the existence and uniqueness of reaction diffusion equations refer to, e.g., [Gri96] and on the existence and uniqueness of parabolic equations to [Hen81].

To show the positivity of our model, we proceed according to [ES10].

First of all, we want to rewrite our model. The model is therefore identified as a semi-linear parabolic system of equations, because the equations are linear in the higher order derivatives.

With the assumption of a spatially decaying solution the above derived model can be rewritten in the following form:

$$\begin{cases} \partial_t u = D\partial_{xx}u - a\partial_x u + f(u) & (t_0, t_{end}] \times [0, \infty) \\ u|_{t=t_0} = u_0 & t_0 \times [0, \infty) \\ a_1 u + a_2\, \partial_x u|_{x=0} = g & (t_0, t_{end}] \times 0 \\ \lim\limits_{x\to\infty} u = 0 & (t_0, t_{end}], \end{cases} \tag{7.1}$$

where $u = (B_{ext}, B_{int}, A, N_{ext}, N_{int})^T$, $D = (D_{B_{ext}}, D_{B_{int}}, D_A, D_{N_{ext}}, D_{N_{int}})^T$, $a = (v_f, 0, 0, v_f, 0)^T$, $a_1 = (0, 0, 0, 1, 0)^T$, $a_2 = (1, 1, 1, 0, 1)^T$, $g = (0, 0, 0, n_{inflow}, 0)^T$ and

$$f(u) = \begin{pmatrix} -\frac{c_b}{\eta} e^{-cB_{int}} B_{ext} + \frac{c_A}{\eta} B_{int} \frac{A}{A_{thr1}+A} - \gamma_f B_{ext} \\ c_b e^{-cB_{int}} B_{ext} - c_A B_{int} \frac{A}{A_{thr1}+A} + \beta_{int} B_{int} \frac{N_{int}}{N_{thr}+N_{int}} \\ B_{int} \left(\alpha_A + \beta_A \frac{A^2}{A_{thr2}^2+A^2} \right) - (\gamma_A + d_v) A \\ -\frac{c_N}{\eta} \left(N_{ext} - N_{int} \right) - \gamma_N N_{ext} \\ c_N \left(N_{ext} - N_{int} \right) - c_1 B_{int} \frac{N_{int}}{N_{thr}+N_{int}} - \gamma_N N_{int} \end{pmatrix}$$

The colonisation term was simplified in this approach to avoid complications that might arise from the integral form of the colonisation term. Here we assume that the bacteria only probe if at the exact spot, where they want to colonise, another bacterium is already situated.
It is easy to verify that the reaction term f satisfies: $f \in C^1(\mathbb{R}^5, \mathbb{R}^5)$.

Definition 7.1.1. *We define the positive cone K^+ by $K^+ := \{u : [0, x_{end}] \to \mathbb{R}^5 \mid u^i \in L^2([0,\infty)), u^i \geq 0$ a.e., $i = 1, \ldots, 5\}$, at which u^i the different components of u are.*

Therefore, $u_0 \in K^+$ means that the initial condition is non-negative for almost every $x \in [0, x_{end}]$.

Some more assumptions have to be made to formulate a theorem concerning the positivity of our model:

Assumption 7.1.1. *All parameters used in model* (7.1) *are non-negative and there exists a unique solution $u \in L^2([0,\infty))$ for all initial conditions $u_0 \in K^+$.*

Hence, we arrive at the following theorem:

Theorem 7.1.1 (**Positivity**)**.** *Let assumption 7.1.1 be fulfilled. Furthermore, we assume that the initial condition $u_0 \in K^+$ satisfies the boundary conditions of model* (7.1).
Then, our model has a non-negative solution $u \in L^2([0,\infty))$ for all times $t \in [t_0, t_{end}]$ in terms of the L^2-norm.

Proof. First of all, we want to give a short outline of the proof. In a first step, the solution will be divided into a positive and a negative part. After that an estimate on the derivative with respect to time of the negative part of the solution will be achieved. At last, Gronwall's Lemma (Theorem 2.3.2) and the uniqueness of the solution is used to bring about the sought after result.

As already mentioned, we start by dividing each component of our solution u into two parts: the positive part $u_+^i := max\{0, u^i\}$ and the negative part $u_-^i := max\{-u^i, 0\}$ for $i = 1, \ldots, 5$. The complete positive part of the solution is therefore defined as $u_+ := (u_+^1, \ldots, u_+^5)^T$ and the negative part correspondingly.

This leads to the following results concerning the negative and positive parts: $u^i = u^i_+ - u^i_-$, $|u^i| = u^i_+ + u^i_-$, $u^i_+ u^i_- = 0$. We also know that for $u \in H^1([0,\infty))$ it holds that $u_+, u_- \in H^1([0,\infty))$. The space $H^1([0,\infty))$ is a Sobolev space. For more information on Sobolev spaces, refer to, e.g., [Eva10]. A result for the derivative with respect to x that can be easily attained, is:

$$\partial_x u^i_+ = \begin{cases} \partial_x u^i & \text{if } u^i_+ > 0 \\ 0 & \text{else} \end{cases} \quad \text{and} \quad \partial_x u^i_- = \begin{cases} -\partial_x u^i & \text{if } u^i_- > 0 \\ 0 & \text{else} \end{cases}$$

This is obviously also true for derivatives with respect to time.
Thus we get: $\partial_x u^i_- u^i_+ = \partial_x u^i_+ u^i_- = \partial_t u^i_- u^i_+ = \partial_t u^i_+ u^i_- = 0$.
After the positive, respectively the negative part, of the solution has been introduced, we now want to get an *a priori* estimate of the derivative with respect to time of all components u^i_-. Therefore, we write our governing equation, shown in (7.1), componentwise, multiply each resulting equation by the respective component u^i_- and integrate over our space domain:

$$\int_0^\infty \partial_t u^i u^i_- dx = \int_0^\infty D_i \partial_{xx} u^i u^i_- dx - \int_0^\infty a_i \partial_x u^i u^i_- dx + \int_0^\infty f_i(u) u^i_- dx \tag{7.2}$$

Each term of the above integral equation is now examined separately.
One can rewrite the first term in the following way:

$$\int_0^\infty \partial_t u^i u^i_- dx = \int_0^\infty \partial_t (u^i_+ - u^i_-) u^i_- dx = -\int_0^\infty \partial_t u^i_- u^i_- dx = -\frac{1}{2}\partial_t \left\| u^i_- \right\|^2_{L^2([0,\infty))}$$

To rewrite the diffusion term, we use integration by parts:

$$D_i \int_0^\infty \partial_{xx} u^i u^i_- dx = -D_i \int_0^\infty \partial_{xx} u^i_- u^i_- dx \overset{p.I.}{=} -D_i \partial_x u^i_- \; u^i_-\big|_{x=0}^\infty + D_i \left\| \partial_x u^i_- \right\|^2_{L^2([0,\infty))}$$

The next term that will be dealt with, is the advection term. Again, using integration by parts will lead to the desired form of the advection term:

$$a_i \int_0^\infty \partial_x u^i u^i_- dx = -a_i \int_0^\infty \partial_x u^i_- u^i_- dx = -\frac{1}{2} a_i \left(u^i_-\right)^2 \Big|_{x=0}^\infty$$

At last, we attend to the reaction term. Here we use that $f \in C^1(\mathbb{R}^5, \mathbb{R}^5)$. This allows us to express the components f_i of our reaction term f using the fundamental theorem of calculus as follows:

$$f_i(u^1, \dots, u^5) = f_i(u^1, \dots, \underbrace{0}_{i}, \dots, u^5) + u^i \int_0^1 \partial_i f_i(u^1, \dots, s u^i, \dots, u^5) ds \quad \forall\, i = \{1, \dots, 5\}$$

Thus, we arrive at an approximation of our last term:

$$\int_0^\infty f_i(u)u_-^i dx = \int_0^\infty u_-^i f_i(u^1,\dots,\underbrace{0}_{i},\dots,u^5)dx - \int_0^\infty (u_-^i)^2 \int_0^1 \partial_i f_i(u^1,\dots,su^i,\dots,u^5)dsdx$$

$$\overset{f\in C^1}{\geq} \int_0^\infty f_i(u^1,\dots,0,\dots,u^5)u_-^i dx - c\left\|u_-^i\right\|^2_{L^2([0,\infty))}$$

Using all the above derived alternative forms of the terms found in equation (7.2), we arrive at the following:

$$\frac{1}{2}\partial_t \left\|u_-^i\right\|^2_{L^2([0,\infty))} + D_i \left\|\partial_x u_-^i\right\|^2_{L^2([0,\infty))} + \frac{1}{2}a_i \left(u_-^i\right)^2\Big|_{x=0}^\infty =$$
$$D_i\, \partial_x u_-^i u_-^i|_{x=0}^\infty + \int_0^\infty \left(u_-^i\right)^2 \int_0^1 \partial_i f_i(u^1,\dots,su^i,\dots,u^5)dsdx - \int_0^\infty u_-^i f_i(u^1,\dots,0,\dots,u^5)ds$$

The scalars D_i and a_i are positive constants and hence the terms on the left hand side of the equation are positive. This and the approximation for the reaction term yields

$$\frac{1}{2}\partial_t \left\|u_-^i\right\|^2_{L^2([0,\infty))} \leq c\left\|u_-^i\right\|^2_{L^2([0,\infty))} + D_i\partial_x u_-^i u_-^i|_{x=0}^\infty - \int_0^\infty u_-^i f_i(u^1,\dots,0,\dots,u^5)ds. \tag{7.3}$$

As we want to apply Gronwall's Lemma to the above inequality, we still have to approximate the remaining unsuitable terms.

First of all, we take a look at the diffusion term. With the assumption that our solution decays to zero when x tends to infinity, we only consider the term $\partial_x u_-^i(0,t)u_-^i(0,t)$. In our model, we have homogeneous Neumann boundary conditions on the left boundary for all substances, but N_{ext}, as the nutrients in the flow have inhomogeneous Dirichlet boundary condition. Therefore, our model has Robin boundary conditions, which can be written as $a_1 u + a_2\, \partial_x u|_{x=0} = g$.

For $i \neq 4$, i.e., all substances but the nutrients in the flow, we get: $\partial_x u_-^i(0,t)u_-^i(0,t) = 0$

As we assumed n_{inflow} to be non-negative, one arrives at $u_-^4(0,t) = g_-^4 = 0$. Thus, the diffusion term from above is equal to zero for all $i \in \{1,\dots,5\}$.

The last term that needs attention, before we are able to apply Gronwall's Lemma, is the integral term in equation (7.3).

Obviously $f_i(u^1,\dots,\underbrace{0}_{i},\dots,u^5) \geq 0$, if f is defined as in model (7.1) and $u^i \geq 0$ for all $i \in \{1,\dots,5\}$.

Under the assumption that $u^i \geq 0$ for all $i \in \{1,\dots,5\}$, we therefore arrive at the following inequality:

$$\partial_t \left\|u_-^i\right\|^2_{L^2([0,\infty))} \leq c_1 \left\|u_-^i\right\|^2_{L^2([0,\infty))}$$

Finally we can use Gronwall's Lemma (Theorem 2.3.2) on this inequality, which leads to $\left\|u_-^i\right\|^2_{L^2([0,\infty))} = 0$.
This accordingly brings us to

$$u_-^i(x,t) = 0 \quad \text{a.e. in } [t_0, t_{end}] \times [0,\infty).$$

Apparently, this would already show our theorem as it means that $u(t,\cdot;u_0) \in K^+$, if $u_0 \in K^+$. Only the assumption on the reaction term still has to be justified.
This is done by considering a modified system

$$\begin{cases} \partial_t \hat{u} = D\partial_{xx}\hat{u} - a\partial_x \hat{u} + \hat{f}(\hat{u}) & (t_0, t_{end}] \times [0,\infty) \\ \hat{u}|_{t=t_0} = u_0 & t_0 \times [0,\infty) \\ \partial_x \hat{u}|_{x=0} = g & (t_0, t_{end}] \times 0 \\ \lim\limits_{x\to\infty} \hat{u} = 0 & (t_0, t_{end}], \end{cases}$$

where the components of the new reaction term $\hat{f}$ are defined as

$$\hat{f}_i(\hat{u}^1,\dots,\hat{u}^5) := f_i(|\hat{u}^1|,\dots,0,\dots,|\hat{u}^5|) + \hat{u}^i \int_0^1 \partial_i f_i(\hat{u}^1,\dots,s\hat{u}^i,\dots,\hat{u}^5)ds.$$

Using all the above derived approximations for the modified model, it is obvious that for a solution $\hat{u}_-^i$ of the modified model, it holds that $\hat{u}_-^i = 0$ a.e. in $[0,\infty)\times[t_0,t_{end}]$, i.e., $\hat{u}(t,\cdot;u_0) \in K^+$ for $u_0 \in K^+$.
Hence we get $\hat{u}^i \geq 0$ a.e. in $[0,\infty) \times [t_0, t_{end}]$. Therefore, $\hat{u}$ is also a solution of our original model (7.1) as $f_i(|\hat{u}^1|,\dots,0,\dots,|\hat{u}^5|) = f_i(\hat{u}^1,\dots,0,\dots,\hat{u}^5)$ in this case. Because of the uniqueness of the solution as demanded in assumption 7.1.1, it follows that $u = \hat{u}$.

Therefore $u \in K^+$, which concludes the proof of our theorem. □

7.2 Pattern formation

Various patterns have been observed to form in plenty of different biological systems. The first one to mathematically analyse the formation of patterns was A.M. Turing. In his excellent work ([Tur52]) a nowadays well-known pattern forming mechanism was examined, i.e., the so-called Turing pattern formation. Less known is another pattern formation, which he already outlined in [Tur52]. It is known as the wave instability pattern formation.
For a pattern arising from a Turing or wave instability, there has to exist at least one stable non-trivial stationary state of the spatially independent model. This is the necessary condition for a pattern formation of the Turing- or wave instability-type. The sufficient condition is the loss of the stability of the stationary state for a certain eigenvalue of Laplace's equation (equation (7.19)), when introducing the spatial coordinates into the model again. A possible shape of the two different patterns can be seen in figures 2.3 and 2.4 in chapter 2.2.2.

A Hopf bifurcation was found in the spatially homogeneous model. This led us to the idea of examining the PDE-model for a possible pattern formation. We were interested to see if the model would show such a behaviour, assuming that there were no influences from the outside, i.e., homogeneous Neumann boundary conditions on all boundaries.

In this thesis the system is simplified to a three-component model to analyse for a possible pattern formation. We will check if the necessary and sufficient conditions of the Turing mechanism as well as of the wave instability pattern formation are fulfilled.

7.2.1 Simplification of the model

Before we can start to check for any conditions on the formation of patterns, our model has to be simplified such that it can be handled analytically.

Again, we use the simplification - as already seen in chapter 7.1 - that for the recolonisation of the biofilm only bacteria at exactly the site of recolonisation are relevant and not the bacteria upstream as well.

The biggest simplification of our model is the assumption of fast and slow processes within our biological system, which we consider next.

We assume that movement due to the flow and diffusion of B_{ext} are considerably slower than the reaction terms. This lets us rewrite equation (6.2) in terms of a small parameter ϵ:

$$\epsilon\frac{\partial B_{ext}}{\partial t} = \epsilon D_{B_{ext}}\frac{\partial^2 B_{ext}}{\partial x^2} - \epsilon v_f\frac{\partial B_{ext}}{\partial x} - \frac{c_b}{\eta}e^{-cB_{int}}B_{ext} + \frac{c_A}{\eta}B_{int}\frac{A}{A_{thr1}+A} - \gamma_f B_{ext}$$

For $\epsilon \to 0$ we arrive at an algebraic equation, which can be solved for B_{ext}:

$$B_{ext} = \frac{e^{cB_{int}}}{c_b + \eta\gamma_f e^{cB_{int}}} c_A B_{int} \frac{A}{A_{thr1} + A}$$

Using this result in the governing equation for B_{int} leads to:

$$\frac{\partial B_{int}}{\partial t} = D_{B_{int}} \frac{\partial^2 B_{int}}{\partial x^2} + c_b e^{-cB_{int}} \left(\frac{e^{cB_{int}}}{c_b + \eta\gamma_f e^{cB_{int}}} c_A B_{int} \frac{A}{A_{thr1} + A} \right) - c_A B_{int} \frac{A}{A_{thr1} + A} + \beta_{int} B_{int} \frac{N_{int}}{N_{thr} + N_{int}}$$

This gives a modified governing equation for the bacteria in the biofilm:

$$\frac{\partial B_{int}}{\partial t} = D_{B_{int}} \frac{\partial^2 B_{int}}{\partial x^2} - \frac{\eta\gamma_f e^{cB_{int}}}{c_b + \eta\gamma_f e^{cB_{int}}} + \beta_{int} B_{int} \frac{N_{int}}{N_{thr} + N_{int}}$$

The same assumptions are used for the nutrients in the flow and a basal nutrient production rate n_0 is included such that a trivial stationary state exists, which is necessary from a biological point of view. The parameter n_0 is already known from the model, where a homogeneous distribution of all substances over space was assumed. This yields:

$$\epsilon \frac{\partial N_{ext}}{\partial t} = \epsilon \frac{\partial^2 N_{ext}}{\partial x^2} - \epsilon v_f \frac{\partial N_{ext}}{\partial x} - \frac{c_N}{\eta}(N_{ext} - N_{int}) - \gamma_N N_{ext} + n_0$$

Therefore, assuming $\epsilon \to 0$, this equation results in the following expression for the nutrients in the flow:

$$N_{ext} = \frac{c_N}{c_N + \eta\gamma_N} N_{int} + \frac{\eta n_0}{c_N + \eta\gamma_N}$$

This expression used in the governing equation for the nutrients in the biofilm leads to

$$\frac{\partial N_{int}}{\partial t} = D_{N_{int}} \frac{\partial^2 N_{int}}{\partial x^2} + c_N \left(\left(\frac{c_N}{c_N + \eta\gamma_N} N_{int} + \frac{\eta n_0}{c_N + \eta\gamma_N} \right) - N_{int} \right) - \gamma_N N_{int} - c_1 B_{int} \frac{N_{int}}{N_{thr} + N_{int}}.$$

Some straight forward calculations admit us to write the governing equation for N_{int} in the following way:

$$\frac{\partial N_{int}}{\partial t} = D_{N_{int}} \frac{\partial^2 N_{int}}{\partial x^2} + M_1 - M_2 N_{int} - c_1 B_{int} \frac{N_{int}}{N_{thr} + N_{int}},$$

where $M_1 := \frac{\eta c_N n_0}{c_N+\eta\gamma_N} \geq 0$ and $M_2 := \frac{\gamma_N(c_N+\eta c_N+\eta\gamma_N)}{c_N+\eta\gamma_N} \geq 0$.

Considering all the above, we arrive at a reduced model, where we also assume homogeneous Neumann boundary conditions and, in contrast to the original model (6.3) - (6.5), a bounded domain:

$$\begin{aligned}
\frac{\partial B}{\partial t} =& D_B \frac{\partial^2 B}{\partial x^2} + \beta_{int} B \frac{N}{N_{thr}+N} - \frac{\eta\gamma_f e^{cB}}{c_b+\eta\gamma_f e^{cB}} c_A B \frac{A}{A_{thr1}+A} \\
\frac{\partial A}{\partial t} =& D_A \frac{\partial^2 A}{\partial x^2} + B\left(\alpha_A + \beta_A \frac{A^2}{A_{thr2}^2+A^2}\right) - (\gamma_A + d_v)\, A \\
\frac{\partial N}{\partial t} =& D_N \frac{\partial^2 N}{\partial x^2} + M_1 - M_2 N - c_1 B \frac{N}{N_{thr}+N},
\end{aligned}$$

with the boundary conditions

$$\frac{\partial B(t,0)}{\partial x} = \frac{\partial A(t,0)}{\partial x} = \frac{\partial N(t,0)}{\partial x} = \frac{\partial B(t,x_{end})}{\partial x} = \frac{\partial A(t,x_{end})}{\partial x} = \frac{\partial N(t,x_{end})}{\partial x} = 0 \tag{7.4}$$

and initial conditions

$$B(0,x) = B_0(x),\ A(0,x) = A_0(x),\ N(0,x) = N_0(x), \tag{7.5}$$

where the subscripts were dropped for reasons of brevity.

Even though the model has been simplified to a three component model, it is still not possible to calculate the stationary states analytically. Thus, the model needs some more adjustments to analyse it for a possible pattern formation.

The first assumption in terms of simplifying the model even further is to linearise the term $\frac{N}{N_{thr}+N}$ about 0. This is justified, when accepting the fact that there are little nutrients available for the bacteria in a non-trivial stationary phase.

Linearisation yields:

$$\frac{N}{N_{thr}+N} \approx \frac{N}{N_{thr}}$$

The next term that will be approximated, is the positive feedback of the AHL-production due to quorum sensing. The original term is a sigmoidal function with respect to the present AHL-concentration. This will be approximated via a jump function as represented in figure 7.1(a).

The original production term reads $h(A) := \alpha_A + \beta_A \frac{A^2}{A_{thr,2}^2+A^2}$ and the simplified term

$$0 \leq g(A) := \begin{cases} \alpha_A & \text{if } A \leq A_{thr,2} \\ \alpha_A + \beta_A & \text{if } A > A_{thr,2}. \end{cases}$$

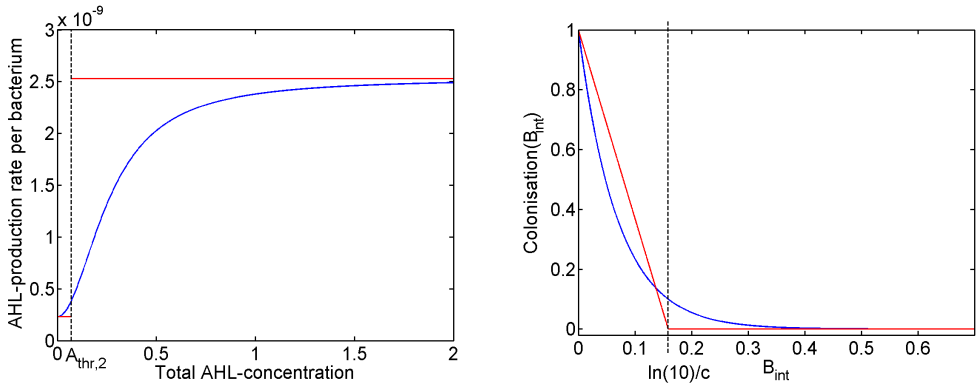

(a) (b)

Figure 7.1: (a) Original AHL-production rate with respect to the present AHL-concentration is shown in blue and the approximated production rate (jump function) in red. (b) In blue the term e^{-cB} is shown, which is part of the colonisation of the biofilm by bacteria from the flow. The approximation used in this section is represented by the red line.

In contrast to the colonisation term below, we use a jump function to approximate the production rate; otherwise we cannot analytically calculate the stationary states. In the following we will always assume the system to be either activated or not. Hence, the AHL-concentration is either small or high. Therefore, the AHL-concentration is far away from A_{thr2} and can be approximated via our jump function.

The last term that has to be coped with, is the colonisation term. As it is exponentially decaying, it is hard to analytically work with. It is approximated by a straight line for small densities of bacteria in the biofilm, which basically means, if there are no bacteria in the biofilm a colonisation is possible. For higher densities of B_{int} the term is approximated by zero, i.e., as soon as bacteria have settled in the biofilm at a certain site, there is no colonisation at this site:

$$e^{-cB} \approx f(B) := \begin{cases} 1 - \dfrac{c}{\ln 10} B & \text{if } B \leq \dfrac{\ln 10}{c} \\ 0 & \text{if } B > \dfrac{\ln 10}{c} \end{cases}$$

The parameter c is assumed to be rather big such that there is no colonisation of the biofilm by bacteria from the flow, if there are other bacteria already present at the specified place. Thus, the decay is fast and our approximation is justified.

Finally, we can formulate our reduced and simplified model, where the boundary and initial conditions (Eq.(7.4) and Eq.(7.5)) persist:

$$\begin{aligned}
\frac{\partial B}{\partial t} &= D_B \frac{\partial^2 B}{\partial x^2} - \frac{\eta\gamma_f}{c_b f(B) + \eta\gamma_f} c_A B \frac{A}{A_{thr,1} + A} + \beta_{int} B \frac{N}{N_{thr}} \\
\frac{\partial A}{\partial t} &= D_A \frac{\partial^2 A}{\partial x^2} + Bg(A) - (\gamma_A + d_v)A \\
\frac{\partial N}{\partial t} &= D_N \frac{\partial^2 N}{\partial x^2} + M_1 - M_2 N - c_1 B \frac{N}{N_{thr}},
\end{aligned} \tag{7.6}$$

where M_1, M_2, $f(B)$ and $g(A)$ are defined as above.

7.2.2 Stationary states of the spatially homogeneous model and their stability

In this part, we calculate the non-trivial stationary states of our reduced model (7.6) with the assumption of a spatially homogeneous distribution of our bacteria and substances and investigate their stability. The governing equations of this model have the following form:

$$\begin{aligned}
\frac{\partial B}{\partial t} &= -\frac{\eta\gamma_f}{c_b f(B) + \eta\gamma_f} c_A B \frac{A}{A_{thr,1} + A} + \beta_{int} B \frac{N}{N_{thr}} =: F(B, A, N) \\
\frac{\partial A}{\partial t} &= Bg(A) - (\gamma_A + d_v)A =: G(B, A, N) \\
\frac{\partial N}{\partial t} &= M_1 - M_2 N - c_1 B \frac{N}{N_{thr}} =: H(B, A, N),
\end{aligned} \tag{7.7}$$

To identify the stationary states we proceed as already seen in chapter 4.2. The stationary states will be denoted by $\bar{X}$.
Therefore, we have to solve the algebraic equations:

$$\beta_{int} \bar{B} \frac{\bar{N}}{N_{thr}} = \frac{\eta\gamma_f}{c_b f(\bar{B}) + \eta\gamma_f} c_A \bar{B} \frac{\bar{A}}{A_{thr,1} + \bar{A}} \tag{7.8}$$

$$\bar{B} g(\bar{A}) = (\gamma_A + d_v)\bar{A} \tag{7.9}$$

$$M_1 = M_2 \bar{N} + c_1 \bar{B} \frac{\bar{N}}{N_{thr}} \tag{7.10}$$

In a first step, equation (7.10) is solved for $\bar{N}$, which leads to:

$$\bar{N} = \frac{M_1 N_{thr}}{M_2 N_{thr} + c_1 \bar{B}} \tag{7.11}$$

Next, the equation for the stationary state of the AHL-concentration (Eq.(7.9)) yields:

$$\bar{A} = \frac{g(\bar{A})}{\gamma_A + d_v} \bar{B} =: M(\bar{A})\bar{B} \tag{7.12}$$

In *Case 1* we will assume that the system is activated in the stationary phase, i.e., the stationary AHL-concentration can be written as $\bar{A} = \frac{\alpha_A+\beta_A}{\gamma_A+d_v}\bar{B}$, because a high number of bacteria leads inevitably to activation. A low density of bacteria will be assumed in *Case 2* and hence, the system is not induced, which in turn leads to: $\bar{A} = \frac{\alpha_A}{\gamma_A+d_v}\bar{B}$.

We are looking for non-trivial stationary states, so $\bar{B} \neq 0$ is a fair assumption. Hence, solving equation (7.8) gives

$$f(\bar{B}) = \frac{\eta\gamma_f \left(c_A N_{thr}\bar{A} - \beta_{int}\left(A_{thr,1} + \bar{A}\right)\bar{N}\right)}{c_b\beta_{int}\bar{N}\left(A_{thr,1} + \bar{A}\right)}. \tag{7.13}$$

Using the derived equalities for $\bar{A}$ and $\bar{N}$ in equation (7.13) yields:

$$f(\bar{B}) = \frac{\eta\gamma_f \left(c_1 c_A M_A \bar{B}^2 + \left(c_A N_{thr} M_2 M_A - \beta_{int} M_1 M_A\right)\bar{B} - \beta_{int} A_{thr,1} M_1\right)}{c_b\beta_{int} M_1 M_A \bar{B} + c_b\beta_{int} A_{thr,1} M_1} \tag{7.14}$$

Now there are two cases, which have to be considered depending on the bacteria in the biofilm.

Case 1: $\bar{B} > \frac{\ln 10}{c}$

We assume that at least one bacterium is in the biofilm. This is equivalent to $f(\bar{B}) = 0$. Thus, equation (7.14), which is a polynomial of second order, can be solved for $\bar{B}$. This gives the non-trivial stationary state:

$$\bar{B}_{1/2} = \frac{\beta_{int} M_1 M_A - c_A M_2 M_A N_{thr}}{2c_1 c_A M_A} \pm \frac{\sqrt{\left(c_A M_2 M_A N_{thr} - \beta_{int} M_1 M_A\right)^2 + 4\beta_{int} c_1 c_A A_{thr,1} M_1 M_A}}{2c_1 c_A M_A}$$

As obviously $\bar{B}_2$ is negative, only $\bar{B}_1$ is a biological relevant stationary state. Therefore, $\bar{B}_2$ will not be considered in the following. The stationary states for the concentration of the nutrients and of AHL are simply obtained by inserting the calculated stationary state $\bar{B}_1$ into equations (7.11) and (7.12).

Case 2: $\bar{B} \leq \frac{\ln 10}{c}$

In this case, there are no bacteria in the biofilm in a stationary phase present, thus $f(\bar{B}) = 1 - \frac{c}{\ln 10}\bar{B}$.

As the explicit solution for the stationary state of the different substances will not be needed for further investigations, it is left out here. It can be calculated using the same techniques as in *Case 1*.

In a next step, we will analyse the stability of our non-trivial stationary states and check for the possibility of a pattern formation. For this purpose we will proceed similar to [Eng94].
First of all, model (7.7) is linearised about the non-trivial stationary state. Therefore, the Jacobian for $\left(\bar{B}, \bar{A}, \bar{N}\right)$ is calculated. The variables of the linearised model will be denoted by small letters. This leads to:

$$\frac{d}{dt}\begin{pmatrix} b \\ a \\ n \end{pmatrix} = L \begin{pmatrix} b \\ a \\ n \end{pmatrix}, \tag{7.15}$$

where L is a real 3×3 matrix. This matrix depends on the different cases for the bacteria in the flow, which were introduced above.
It is a well known fact (e.g., [GH02]) that a linear continuous dynamical system - like system (7.15) - satisfying the following assumption (Assumption 7.2.1) has a trivial stable stationary state. With the theorem of Hartman-Grobman (Theorem 2.3.1) this result can be extended to the nonlinear model (7.7).

Assumption 7.2.1. *All eigenvalues λ_i of L satisfy: $Re\,(\lambda_i) < 0\ \forall i \in \{1, 2, 3\}$.*

For a pattern to form, a non-trivial stable stationary state has to exist in the spatially homogeneous model. Thus we will check, if the above introduced matrix L satisfies assumption 7.2.1. For this purpose the Routh-Hurwitz stability criterion (Theorem 2.3.3) is used.
From the Routh-Hurwitz stability criterion the following three conditions can be deduced (see appendix A for more information):

$$\begin{aligned} \operatorname{tr}(L) &< 0 \\ \det(L) - \operatorname{tr}(L)\mathrm{r}(L) &> 0 \\ \det(L) &< 0, \end{aligned} \tag{7.16}$$

where $\mathrm{r}(L) := \frac{\partial F}{\partial B}\frac{\partial G}{\partial A} - \frac{\partial F}{\partial A}\frac{\partial G}{\partial B} + \frac{\partial F}{\partial B}\frac{\partial H}{\partial N} - \frac{\partial F}{\partial N}\frac{\partial H}{\partial B} + \frac{\partial G}{\partial A}\frac{\partial H}{\partial N} - \frac{\partial G}{\partial N}\frac{\partial H}{\partial A}$.
Those have to be satisfied in order to have only eigenvalues of L with negative real parts.

Case 1: $\bar{B} > \frac{\ln 10}{c}$
In *Case 1* the linearised model (7.15) has the following form:

$$\frac{d}{dt}\begin{pmatrix} b \\ a \\ n \end{pmatrix} = \underbrace{\begin{pmatrix} \frac{\beta_{int}\bar{N}}{N_{thr}} - c_A\frac{\bar{A}}{A_{thr,1}+\bar{A}} & -c_A\bar{B}\frac{A_{thr,1}}{\left(A_{thr,1}+\bar{A}\right)^2} & \beta_{int}\frac{\bar{B}}{N_{thr}} \\ g(\bar{A}) & -(\gamma_A + d_v) & 0 \\ -c_1\frac{\bar{N}}{N_{thr}} & 0 & -\left(M_2 + c_1\frac{\bar{B}}{N_{thr}}\right) \end{pmatrix}}_{=:L_1} \begin{pmatrix} b \\ a \\ n \end{pmatrix}.$$

Under the assumption that all parameters are positive and only considering the signs of the entries of the Jacobian matrix L_1, we arrive at the following representation of the signs of L_1:

$$\begin{pmatrix} 0 & - & + \\ + & - & 0 \\ - & 0 & - \end{pmatrix}, \tag{7.17}$$

where the entry in the top left corner follows directly from equation (7.8).

Now it is easy to verify the conditions shown in (7.16).

While the first and third condition are obviously true, the second one is proven to be valid with straight forward calculations. Therefore, assumption 7.2.1 holds and thus all eigenvalues of L_1 have only negative real parts.

Hence, using the theorem of Hartman-Grobman yields that the non-trivial stationary state of model (7.7) is stable in *Case 1.* This is - as already mentioned - a necessary condition for a Turing pattern to form.

Case 2: $\bar{B} < \frac{\ln 10}{c}$

As the stationary state for *Case 2* is different, the linearisation changes. The Jacobian L_2 now has the form:

$$L_2 := \begin{pmatrix} \frac{\beta_{int}\bar{N}}{N_{thr}} - M(\bar{B})c_A\frac{\bar{A}}{A_{thr,1}+\bar{A}} & -\frac{\gamma_f\eta}{c_b(1-m\bar{B})+\gamma_f\eta}c_A\bar{B}\frac{A_{thr,1}}{\left(A_{thr,1}+\bar{A}\right)^2} & \beta_{int}\frac{\bar{B}}{N_{thr}} \\ \alpha_A & -(\gamma_A+d_v) & 0 \\ -c_1\frac{\bar{N}}{N_{thr}} & 0 & -\left(M_2+c_1\frac{\bar{B}}{N_{thr}}\right) \end{pmatrix},$$

where $m := \frac{c}{\ln 10}$ and $M(B) := \frac{\gamma_f\eta(c_b+\gamma_f\eta)}{\left(c_b(1-mB)+\gamma_f\eta\right)^2}$.

Again we want to write the Jacobian in a form, in which only the signs of its entries are considered. Only the first two entries in the first row are different to *Case 1.* The second entry is obviously negative as $1 - m\bar{B} > 0$.

Therefore, the only entry that has to be coped with, is the one in the top left corner:

$$\begin{aligned} \beta_{int}\bar{B}\frac{\bar{N}}{N_{thr}} &\overset{(7.8)}{=} \frac{\eta\gamma_f}{c_b(1-m\bar{B})+\eta\gamma_f}c_A\bar{B}\frac{\bar{A}}{A_{thr,1}+\bar{A}} < \\ &< \underbrace{\frac{c_b+\eta\gamma_f}{c_b+\eta\gamma_f-c_bm\bar{B}}}_{>1}\cdot\frac{\eta\gamma_f}{c_b(1-m\bar{B})+\eta\gamma_f}c_A\bar{B}\frac{\bar{A}}{A_{thr,1}+\bar{A}} = M(\bar{B})c_A\bar{B}\frac{\bar{A}}{A_{thr,1}+\bar{A}}. \end{aligned}$$

Now we arrive at the following for L_2:

$$\begin{pmatrix} - & - & + \\ + & - & 0 \\ - & 0 & - \end{pmatrix} \tag{7.18}$$

Thus, all three conditions are fulfilled and hence all eigenvalues of L_2 have negative real parts. Correspondingly the non-trivial stationary state of model (7.7) is stable.

7.2.3 Diffusion-driven instability I (Turing instability)

Since there exists a non-trivial stable stationary state, the next step is to check for the possibility of a Turing bifurcation, i.e., the stationary state becomes instable, when introducing diffusion into model (7.15).
We follow [Mur03] to arrive at a characteristic equation for the eigenvalue λ of the spatially homogeneous problem.
In a first step, we consider the time-independent solution $W(x)$ of the spatial eigenvalue problem:

$$\begin{aligned} \partial_{xx} W_i + k^2 W_i = 0 \quad & \forall\, i \in \{1,2,3\} \\ \partial_x W_i = 0 \quad & \forall\, i \in \{1,2,3\},\ \forall\, x \in \{0, x_{end}\} \end{aligned} \tag{7.19}$$

The eigenfunctions of this problem have the form:

$$W(x) = \begin{pmatrix} c_1 \cos\left(\frac{n\pi x}{x_{end}}\right) \\ c_2 \cos\left(\frac{n\pi x}{x_{end}}\right) \\ c_3 \cos\left(\frac{n\pi x}{x_{end}}\right) \end{pmatrix}, \quad c_1, c_2, c_3 \in \mathbb{R}, n \in \mathbb{Z}$$

The eigenvalues corresponding to the above eigenfunctions are: $k = \frac{n\pi}{x_{end}}$. Sometimes the eigenvalue k will be referred to as wavenumber.
This lets us define the following function in dependence on the eigenfunctions as:

$$W_k(x) := \begin{pmatrix} c_1 \cos(kx) \\ c_2 \cos(kx) \\ c_3 \cos(kx) \end{pmatrix}$$

In this approach the time component of our system was neglected. This changes, when linear combinations of $W_k(x)$ are used to define:

$$w(x,t) := \sum_k c_k e^{\lambda t} W_k(x),\ c_k \in \mathbb{R}^3$$

Be aware of the difference between the c_k's in the definition of $w(x,t)$ and the parameters c_1, c_2 and c_3 from above.
Obviously $w(x,t)$ is a solution of the linearised problem:

$$\begin{aligned} w_t = Lw + D\partial_x w \quad & [0, x_{end}] \times [t_0, t_{end}] \\ w(x,0) = w_0(x) \quad & \forall x \in [0, x_{end}] \\ \partial_x w(0,t) = \partial_x w(x_{end}, t) = 0 \quad & \forall t \in [t, t_{end}], \end{aligned} \tag{7.20}$$

where $D = \begin{pmatrix} D_B & 0 & 0 \\ 0 & D_A & 0 \\ 0 & 0 & D_N \end{pmatrix}$ and L is the matrix defined in model (7.15).

Using the definition of $w(x,t)$ in problem (7.20), yields for each k:

$$\lambda W_k = LW_k + D\partial_{xx}W_k \overset{(7.19)}{=} LW_k - k^2 DW_k$$

As we are looking for non-trivial functions W_k, the eigenvalue λ of the space independent eigenvalue problem is determined by the roots of the characteristic equation:

$$\det(L - k^2 D - \lambda I) = 0 \tag{7.21}$$

Some cumbersome but straight forward calculations (as shown in appendix A) lead to the following polynomial:

$$\lambda^3 + a_1\lambda^2 + a_2\lambda + a_3 = 0, \tag{7.22}$$

with

$$\begin{aligned}
a_1 &= k^2(D_B + D_A + D_N) - \mathrm{tr}(L) \\
a_2 &= k^4(D_B D_A + D_B D_N + D_A D_N) \\
&\quad - k^2\left(\frac{\partial F}{\partial B}(D_A + D_N) + \frac{\partial G}{\partial A}(D_B + D_N) + \frac{\partial H}{\partial N}(D_B + D_A)\right) + \mathrm{r}(L) =: Q(k^2) \\
a_3 &= b_0 k^6 - b_1 k^4 + b_2 k^2 - \det(L) =: P(k^2),
\end{aligned}$$

where

$$\begin{aligned}
b_0 &= D_B D_A D_N \\
b_1 &= \frac{\partial F}{\partial B} D_A D_N + \frac{\partial G}{\partial A} D_B D_N + \frac{\partial H}{\partial N} D_B D_A \\
b_2 &= D_B\left(\frac{\partial G}{\partial A}\frac{\partial H}{\partial N} - \frac{\partial G}{\partial N}\frac{\partial H}{\partial A}\right) + D_A\left(\frac{\partial F}{\partial B}\frac{\partial H}{\partial N} - \frac{\partial F}{\partial N}\frac{\partial H}{\partial B}\right) + D_N\left(\frac{\partial F}{\partial B}\frac{\partial G}{\partial A} - \frac{\partial F}{\partial A}\frac{\partial G}{\partial B}\right).
\end{aligned}$$

To apply the Routh-Hurwitz stability criterion once more, three conditions have to be satisfied:

$$\begin{aligned}
a_1 &> 0 \\
a_3 &> 0 \\
a_1 a_2 &> a_3
\end{aligned} \tag{7.23}$$

Because of $\mathrm{tr}(L) < 0$ the first condition is satisfied.

All three conditions can only be fulfilled, if $a_2 \in \mathbb{R}_+ \backslash \{0\}$.

As a_2 is a parabola opening up as a function of k^2, the roots of $Q(k^2)$ in terms of k^2 have either to be negative or to have an imaginary part. This is true due to the fact that $a_2(k^2 = 0) = \mathrm{r}(L) > 0$ as seen in the previous subsection.

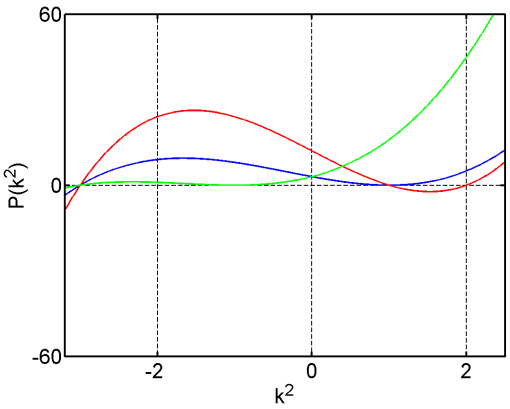

Figure 7.2: Possible shapes for $P(k^2)$ depending on different values for b_1, b_2 and b_3

The roots of $Q(k^2)$ are:

$$k^2 = \frac{\left(\frac{\partial F}{\partial B}(D_A + D_N) + \frac{\partial G}{\partial A}(D_B + D_N) + \frac{\partial H}{\partial N}(D_B + D_A)\right)}{2(D_B D_A + D_B D_N + D_A D_N)} \pm$$
$$\frac{\sqrt{\left(\frac{\partial F}{\partial B}(D_A + D_N) + \frac{\partial G}{\partial A}(D_B + D_N) + \frac{\partial H}{\partial N}(D_B + D_A)\right)^2 - 4\mathrm{r}(L)(D_B D_A + D_B D_N + D_A D_N)}}{2(D_B D_A + D_B D_N + D_A D_N)}$$

Referring to (7.17) and (7.18), one can check that the above mentioned proposition that the roots of $Q(k^2)$ are either negative or have imaginary parts, is correct.

So far, all conditions of the Routh-Hurwitz stability criterion are fulfilled. For a Turing instability to occur, one condition, namely $a_3 > 0$, has to be dissatisfied for at least one wavenumber $k_c^2 > 0$.

We already know that $a_3(k^2 = 0) > 0$. Hence, some possible shapes of the polynomial $a_3 = P(k^2)$ of third order can be seen in figure 7.2. The polynomial crosses the y-axis at $-\det(L)$.

For the Turing instability $P(k^2)$ needs to have positive as well as negative values for $k^2 > 0$, i.e., $\min_{k^2} P(k^2) < 0$. So we are looking for a minimum of $P(k^2)$.

As $P(k^2) = b_0 k^6 - b_1 k^4 + b_2 k^2 - \det(L)$, the first derivative with respect to k^2 can be easily calculated and has the following form:

$$\frac{dP(k^2)}{dk^2} = 3b_0 k^4 - 2b_1 k^2 + b_2 \stackrel{!}{=} 0$$

Setting the derivative to zero, lets us determine the position of the minimum.

$$\frac{dP(k^2)}{dk^2} = 0 \;\Leftrightarrow\; k^2 = \frac{b_1 \pm \sqrt{b_1^2 - 3b_0 b_2}}{3b_0} \tag{7.24}$$

It is a polynomial of second order and hence has two roots (Eq. (7.24)). Taking a look at figure 7.2 tells us that the smaller k^2-value gives the position of the local maximum, whereas the larger one gives the position of the local minimum.
We will denote the wavenumber, which coincides with the local minimum of $P(k^2)$ with k_c^2. This wavenumber has to be real and positive and $P(k_c^2)$ has to be negative in order to get a diffusion-driven instability.

Firstly, the requirements for k_c^2 are tested. In order to have a positive and real k_c^2, we need:

$$b_1^2 > 3b_0b_2 \text{ and}$$
$$b_1 > 0 \text{ or } b_2 < 0$$

Those have to be evaluated in a next step. For this purpose the by now well-known cases are examined separately:

Case 1: $\bar{B} > \frac{\ln 10}{c}$
The definition of b_1 was: $b_1 = \frac{\partial F}{\partial B}D_AD_N + \frac{\partial G}{\partial A}D_BD_N + \frac{\partial H}{\partial N}D_BD_A$
From the definition of L_1 or (7.17) we know that $\frac{\partial F}{\partial B} = 0$, $\frac{\partial G}{\partial A} < 0$ and $\frac{\partial H}{\partial N} < 0$. Also we chose all parameters to be non-negative and at least one diffusion-coefficient has to be positive. Hence we get: $b_1 < 0$.

As b_1 does not satisfy the above, b_2 is tested next. Its definition is:

$$b_2 := D_B\Big(\underbrace{\frac{\partial G}{\partial A}\frac{\partial H}{\partial N}}_{>0} - \underbrace{\frac{\partial G}{\partial N}\frac{\partial H}{\partial A}}_{=0}\Big) + D_A\Big(\underbrace{\frac{\partial F}{\partial B}\frac{\partial H}{\partial N}}_{=0} - \underbrace{\frac{\partial F}{\partial N}\frac{\partial H}{\partial B}}_{<0}\Big) + D_N\Big(\underbrace{\frac{\partial F}{\partial B}\frac{\partial G}{\partial A}}_{=0} - \underbrace{\frac{\partial F}{\partial A}\frac{\partial G}{\partial B}}_{<0}\Big) > 0$$

As the required conditions on b_1 and b_2 are not fulfilled, it is not possible to show a Turing instability with this approach in *Case 1.*

Case 2: $\bar{B} < \frac{\ln 10}{c}$
In *Case 2* the same problem arises as $b_1 < 0$ and $b_2 > 0$ (compare definition of b_1 and b_2 and (7.18)). Hence, the sufficient conditions for a Turing pattern to arise are fulfilled neither.

An outline on which conditions have to be fulfilled for a three-dimensional system such that a Turing pattern can form, is found in appendix A.

7.2.4 Diffusion-driven instability II (Wave instability)

Most parts from section 7.2.3 can be used here as well. The only difference is that we are looking for a possible Hopf bifurcation - not a saddle-node bifurcation - this time, which occurs when assuming a non-homogeneous distribution of the substances over

space. We use the idea formulated in [HNA13] to state a sufficient condition for a wave instability.

The characteristic equation, which is shown in equation (7.21), stays the same. As we are looking for a Hopf bifurcation, the conditions shown in (7.23) still have to be fulfilled.
In the previous section, we looked at the transition of a_3 from positive to negative values. Now theorem 2.3.4 and the afterwards derived condition on the coefficients are used to arrive at the conclusion that there has to be a transition of $P_1(k^2) := a_1(k^2)a_2(k^2) - a_3(k^2)$ from positive to negative values, while a_3 has to stay positive. Thus we need:

$$\exists\ k_c^2 > 0 : \min_{k_c^2} P_1(k_c^2) < 0 \tag{7.25}$$

The actual form of $P_1(k^2)$ can be found in appendix A. To find the position of the local minimum, i.e., k_c^2, the first derivative of $P_1(k^2)$ with respect to k^2 has to be calculated. From appendix A, we already know: $P_1(k^2) = ak^6 + bk^4 + ck^2 + d$.
Therefore we get:

$$\frac{dP_1(k^2)}{k^2} = 3ak^4 + 2bk^2 + c$$

For the two different cases of non-trivial stable stationary states, one can calculate that: $a > 0$, $b > 0$ and $c > 0$.
The first derivative is a parabola opening up, which means that its roots, if real, can only be negative. Hence, there exists no k_c^2 such that condition (7.25) is fulfilled.

The breach of condition (7.25) does not allow us to state the possibility of a pattern formation caused by a wave instability as the sufficient condition for such a pattern formation is not satisfied.

7.3 Summary of the achieved results

In this chapter, we were able to show the positivity of the solutions of our spatially inhomogeneous model under a few assumptions.
After we simplified our model, we investigated it for a possible pattern formation be it of the Turing- or the wave instability-type. While the necessary condition is satisfied, the sufficient condition introduced in this thesis is never fulfilled as long as the parameters are non-negative. Even though this is not a proof that there exists no pattern, it indicates that there might not be a pattern. Biologically this would mean that there is no stationary state, where separate colonies coexist. So if one would let the experiment run for a long time, there will be either no bacteria in the biofilm or the biofilm will be at its capacity with bacteria or the biofilm will change its bacterial density periodically as seen in chapter 5, where a spatially homogeneous distribution was assumed.

8 Simulations on the PDE-model

In this chapter, the simulations of the model explained in chapter 6 will be conducted. For this purpose, the system has to be discretised first, which is done in the following section. Afterwards, suitable parameter values have to be chosen. Finally, the simulations can be carried out. The figures in section 8.3 were done with Matlab ([Mat10]).

8.1 Discretisation of the PDE-model

In order to simulate our PDE-model (equations (6.3), (6.4) and (6.5)), it has to be discretised. In this work we follow [Bra11] to arrive at a suitable approximation of our governing equations to simulate them. More on the discretisation of reaction-diffusion-advection models can be found in [HV03].
We will discretise our model with finite differences in a semi-implicit fashion; while we consider the reaction terms explicitly, i.e., in the current time step of evaluation, the diffusion and advection terms are considered implicitly, i.e., in the next time step.

At first, the domain of interest of the model is divided into a grid. The grid will be equidistant in both space as well as time. While the dimension of time is split into Nt parts of size Δt, the space-dimension is split into Nx parts of size Δx.
The equidistant grid is chosen as it is easier to implement and not as time consuming during the simulation as a non-equidistant grid. A representation of the grid is seen in figure 8.1.

Next, we introduce the notation, which will be used throughout this chapter:
For reasons of readability we will not refer to the different substances and bacteria in the theoretical explanation of the discretisation explicitly, but to a variable called u.
The numerical approximation of $u(t_k)$ is u^k, i.e., u at time-point t_k and the numerical approximation of $u(x_j)$ is u_j, i.e., u at position x_j.

The three most common schemes in finite differences to approximate derivatives of first or second order are: *forward difference scheme*, *backward difference scheme* and *central difference scheme*.
We use the *forward difference scheme* to discretise the derivative with respect to time, the *backward difference scheme* for the advection term and the *central difference scheme* for the diffusion term.

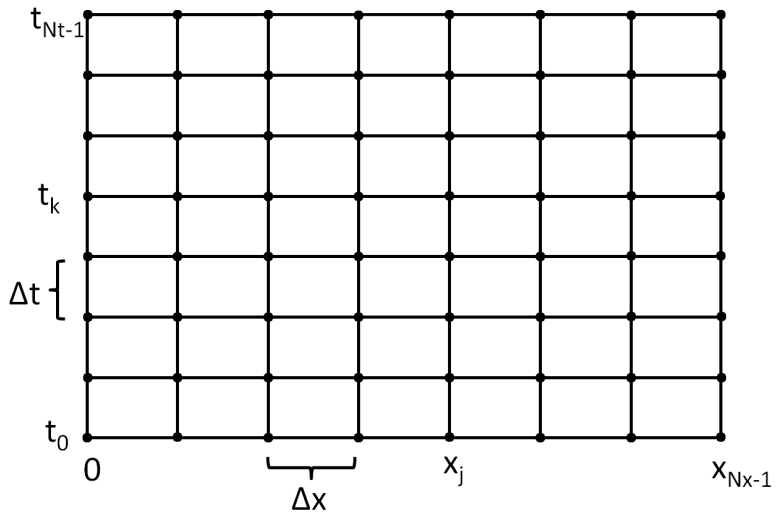

Figure 8.1: Grid of the domain for the simulation of the PDE-model

For more information on the different schemes used for the different derivatives please refer to [Bra11] or [HV03].

8.1.1 Approximation of the derivative with respect to time

The first discretisation to be considered is the derivative of u with respect to time. As mentioned above the *forward difference scheme* is used. Hereby u^{k+1} is represented using a Taylor-series expansion about time t_k, i.e.,

$$u^{k+1} = u^k + \Delta t \frac{\partial u(t_k)}{\partial t} + O((\Delta t)^2).$$

Rearranging the equation leads to:

$$\frac{u^{k+1} - u^k}{\Delta t} = \frac{\partial u(t_k)}{\partial t} + O(\Delta t)$$

The term on the left hand side can now be used as an approximation of first order of the derivative of u with respect to time. The truncation error - when neglecting higher order terms - is of magnitude Δt. This discretisation is called - as already mentioned above - *forward difference scheme*. It will be used to discretise our time-derivative.

8.1.2 Approximations of the derivatives with respect to space

The two remaining derivatives in our model both depend on the space variable x. We begin by discretising the first derivative with respect to x.

First derivative: Applying the *backward difference scheme* to the first derivative with respect to space approximates our advection term. For this purpose the Taylor-series expansion of u_{j-1} about x_j is considered:

$$u_{j-1} = u_j - \Delta x \frac{\partial u(x_j)}{\partial x} + \frac{(\Delta x)^2}{2} \cdot \frac{\partial^2 u(x_j)}{\partial x^2} + O((\Delta x)^3)$$

A rearrangement yields:

$$\frac{u_j - u_{j-1}}{\Delta x} = \frac{\partial u(x_j)}{\partial x} - \frac{\Delta x}{2} \cdot \frac{\partial^2 u(x_j)}{\partial x^2} + O((\Delta x)^2) \tag{8.1}$$

The left hand side of equation (8.1) will approximate the advection term later on. Even though the truncation error of the *central difference scheme* is of $O((\Delta x)^2)$ - shown in equation (B.1) in appendix B.1 - and hence better than the one for the *backward difference scheme*, if it is truncated after the first term, it is not applied on our model as it leads to unwanted and unrealistic oscillations ([HV03]). This is why the *backward difference scheme* is used to approximate the advection term in the simulations later on.

Second derivative: The last remaining term to be discretised is the diffusion-term. We approximate it via the *central difference scheme*. The *forward difference scheme* with respect to space - instead of time as above - is needed thereto. Following the idea shown for the time-derivative gives:

$$\frac{u_{j+1} - u_j}{\Delta x} = \frac{\partial u(x_j)}{\partial x} + \frac{\Delta x}{2} \cdot \frac{\partial^2 u(x_j)}{\partial x^2} + O((\Delta x)^2) \tag{8.2}$$

The first derivative disappears when equation (8.1) is subtracted from equation (8.2). Hence, one arrives at the following approximation for the second derivative:

$$\frac{u_{j+1} - 2u_j + u_{j-1}}{(\Delta x)^2} = \frac{\partial^2 u(x_j)}{\partial x^2} + O((\Delta x)^2) \tag{8.3}$$

The left hand side of equation (8.3) is used to approximate the diffusion term.

8.1.3 Discretisation of our model

So far, only the theoretical variable u was used to explain the different schemes on how to discretise a PDE-model for the purpose of simulation. Now the gained knowledge is employed on our model. In a first step, only the inner domain is regarded as on the boundary of the domain the different boundary conditions have to be taken into account. Afterwards, the model is discretised on the boundaries; firstly taken the boundary conditions in the biofilm and last, but not least, the boundary conditions in the flow into account.

Inner domain:
Exemplarily, we will discretise the governing equation for bacteria in the flow. The discretisation for the other substances follows accordingly.

Using the different schemes for the derivatives - as it was explained in the previous part - leads to the following algebraic equation for all $j \in \{1, ..., Nx-2\}$ and $k \in \{1, ..., Nt-1\}$:

$$\frac{B^{k+1}_{ext,j} - B^k_{ext,j}}{\Delta t} = D_{B_{ext}} \frac{B^{k+1}_{ext,j+1} - 2B^{k+1}_{ext,j} + B^{k+1}_{ext,j-1}}{(\Delta x)^2} - v_f \frac{B^{k+1}_{ext,j} - B^{k+1}_{ext,j-1}}{\Delta x} + \\ + \frac{c_A}{\eta} B^k_{int,j} \frac{A^k_j}{A_{thr1} + A^k_j} - \frac{c_b}{\eta} \operatorname{col}(B^k_{int,j}) B^k_{ext,j} - \gamma_f B^k_{ext,j},$$

where the integral of the colonisation term - as seen in equations (6.1) and (6.2) - is approximated by the function $\operatorname{col}(B^k_{int,j})$, which is defined as

$$\operatorname{col}(B^k_{int,j}) := \begin{cases} 1 & \text{if } \sum_{i=h_2(j)}^{j} B^k_{int,i} \leq 1.2 \cdot 10^{10} \frac{Bact}{ml} \\ 0 & \text{else,} \end{cases}$$

where $h_2(j) := \begin{cases} j - \lfloor \delta_b / \Delta x \rfloor & \text{if } j - \lfloor \delta_b / \Delta x \rfloor > 0 \\ 0 & \text{else} \end{cases}$ and $c = 1$.
As we are using a deterministic approach, we get an average of a stochastic simulation. When there is a bacterium in a distance of δ_b upstream, then there should be no colonisation. The density of $1.2 \cdot 10^{10} \frac{Bact}{ml}$ is equivalent to one bacterium in the biofilm, thus we use this value as a threshold for the above defined function col.
Also remember that the reaction terms are evaluated at time t_k.

Rearranging this equation such that all terms of time point t_{k+1} are on the left hand side, gives:

$$B^{k+1}_{ext,j} - \frac{\Delta t}{(\Delta x)^2} D_{B_{ext}} \left(B^{k+1}_{ext,j+1} - 2B^{k+1}_{ext,j} + B^{k+1}_{ext,j-1} \right) + \frac{\Delta t}{\Delta x} v_f \left(B^{k+1}_{ext,j} - B^{k+1}_{ext,j-1} \right) = \\ = B^k_{ext,j} + \Delta t \left(-\frac{c_b}{\eta} \operatorname{col}(B^k_{int,j}) B^k_{ext,j} + \frac{c_A}{\eta} B^k_{int,j} \frac{A^k_j}{A_{thr1} + A^k_j} - \gamma_f B^k_{ext,j} \right).$$

The discretised equations of all substances are shown in appendix B.2.

Boundaries:
Obviously for the simulations some boundary conditions (b.c.) have to be formulated. Those depend on the different substances. While for all substances in the

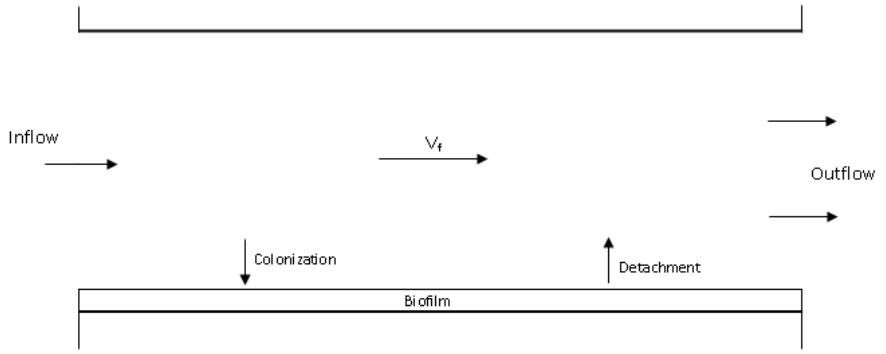

Figure 8.2: Sketch to justify Neumann boundary conditions for the substances in the biofilm

biofilm a homogeneous Neumann boundary condition on the left as well as on the right boundary is assumed, the boundary conditions in the flow have to be chosen more carefully.

Biofilm: First of all, we take a look at the boundary conditions in the biofilm as those are more straight forward than those in the flow. As already mentioned, we are applying homogeneous Neumann boundary conditions, i.e., $\frac{\partial u}{\partial x}\big|_{x=0} = \frac{\partial u}{\partial x}\big|_{x=x_{end}} = 0$.

The biological justification to use Neumann boundary conditions is seen in figure 8.2. In this figure our biological set-up is shown. While the flow moves unhindered through the left and right boundaries of the domain, all substances located in the biofilm can only leave the biofilm by moving into the flow.

Using the above derived ideas to discretise the space derivative, a homogeneous Neumann boundary condition leads to $u_{-1} = u_0$ on the left boundary and to $u_{Nx} = u_{Nx+1}$ on the right boundary.

This yields the following discretised equation for B_{int} at the left boundary, which is shown exemplarily for the discretisation at the boundary of a substance in the biofilm:

$$B_{int,0}^{k+1} - \frac{\Delta t}{(\Delta x)^2} D_{B_{int}} \left(B_{int,1}^{k+1} - B_{int,0}^{k+1} \right) =$$
$$= B_{int,0}^{k} + \Delta t \left(c_b \, \mathrm{col}(B_{int,0}^{k}) B_{ext,0}^{k} - c_A B_{int,0}^{k} \frac{A_0^k}{A_{thr1} + A_0^k} + \beta_{int} B_{int,0}^{k} \frac{N_{int,0}^{k}}{N_{thr} + N_{int,0}^{k}} \right)$$

Both - left and right - boundaries for the substances in the biofilm can be seen in appendix B.2.

Flow: As already mentioned, the boundary conditions in the flow domain have to be chosen carefully. On the left boundary, we assume a homogeneous Neumann boundary condition for the bacteria just as for the substances in the biofilm. It is a reasonable assumption as the flow is really strong and the diffusion of the comparatively large bacteria rather slow. Thus, all the bacteria get washed downstream, if they do not react with a different substance or die, and therefore can not cross the upstream boundary. This idea gives the following discretised equation for B_{ext} on the left boundary:

$$B_{ext,0}^{k+1} - \frac{\Delta t}{(\Delta x)^2} D_{B_{ext}} \left(B_{ext,1}^{k+1} - B_{ext,0}^{k+1} \right) = \\ = B_{ext,0}^{k} + \Delta t \left(-\frac{c_b}{\eta} \operatorname{col}(B_{int,0}^{k}) B_{ext,0}^{k} + \frac{c_A}{\eta} B_{int,0}^{k} \frac{A_0^k}{A_{thr1} + A_0^k} - \gamma_f B_{ext,0}^{k} \right)$$

The only substance not having a homogeneous Neumann boundary condition at the inflow is the nutrient concentration in the flow. The idea that there is at each time-step the same amount of nutrients available at the inflow is translated into a non-homogeneous Dirichlet boundary condition. It is important to use the Dirichlet b.c. as with a Neumann b.c. a constant increase at the inflow would be visible. If we assume for example a liquid saturated with nutrients which flows through our flow chamber, this obviously would not be a reasonable choice. Also one can imagine that the concentration of nutrients at the inflow at a previous time point has been transported further downstream, while nutrients - which were upstream - are now at the inflow.

The non-homogeneous Dirichlet boundary condition leads in a discretised form to

$$N_{ext,-1} = n_{inflow},$$

where $n_{inflow} \in \mathbb{R}_+$ is the constant concentration of nutrients in the flow at $x = 0$. Thus, we arrive at the following equation for N_{ext} at the left boundary:

$$N_{ext,0}^{k+1} - \frac{\Delta t}{(\Delta x)^2} D_{N_{ext}} \left(N_{ext,1}^{k+1} - 2N_{ext,0}^{k+1} \right) + \frac{\Delta t}{\Delta x} v_f N_{ext,0}^{k+1} = \\ = N_{ext,0}^{k} + \Delta t \left(-\frac{c_N}{\eta} \left(N_{ext,0}^{k} - N_{int,0}^{k} \right) - \gamma_N N_{ext,0}^{k} \right) + \left(\frac{\Delta t}{(\Delta x)^2} D_{N_{ext}} + \frac{\Delta t}{\Delta x} v_f \right) n_{inflow}$$

The last boundary condition still missing is the right boundary condition for the two substances in the flow. Referring to figure 8.2 again, yields the idea of an open boundary condition, i.e., the substances are supposed to flow through the boundary unhindered. The realisation of this condition is taken from [PSL97]. In figure 8.3 the basic idea of the open boundary condition is shown. As there should be no change of the substances due to the boundary, the slope left of the boundary has to be the same as right of it.

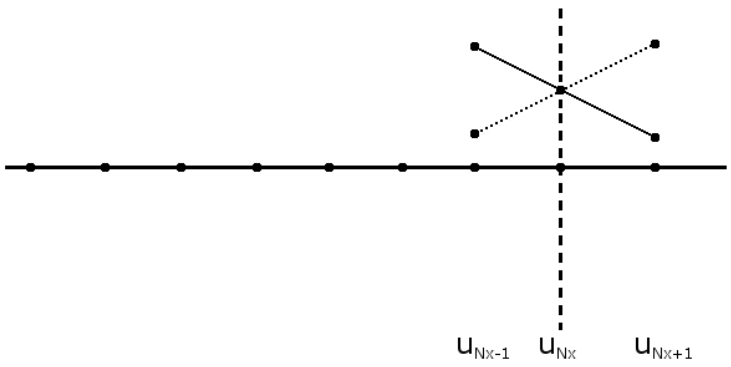

Figure 8.3: Schematic representation of the open boundary condition for the substances in the flow.

Mathematically this is expressed by

$$u_{Nx-1} = \frac{u_{Nx-2} + u_{Nx}}{2}$$

as our grid is supposed to be equidistant.
Thus, the approximation for u_{Nx} reads as follows:

$$u_{Nx} = 2u_{Nx-1} - u_{Nx-2} \tag{8.4}$$

With the approximation seen in equation (8.4), we arrive at the following discretised equation for the nutrients in the flow at the right boundary, which is shown exemplarily:

$$N^{k+1}_{ext,Nx-1} + \frac{\Delta t}{\Delta x} v_f \left(N^{k+1}_{ext,Nx-1} - N^{k+1}_{ext,Nx-2}\right) = \\ = N^{k}_{ext,Nx-1} + \Delta t \left(-\frac{c_N}{\eta}\left(N^{k}_{ext,Nx-1} - N^{k}_{int,Nx-1}\right) - \gamma_N N^{k}_{ext,Nx-1}\right)$$

Using all the above derived discretised equations lets us rewrite our initial model (equations (6.3) - (6.5)) such that we have a system of linear, algebraic equations, which can be solved numerically.

The set of equations can be written as:

$$M_y u^{k+1}_{j,y} = u^{k}_{j,y} + RHS_{k,y} \quad \forall y \in \{B_{ext}, B_{int}, A, N_{ext}, N_{int}\},$$

where $u^k_{j,y}$ the numerical approximation of the component of u represented by y at time t_k and at position x_j, $M_y \in \mathbb{R}^{n \times n}$ the discretisation matrix and $RHS_{k,y}$ the right hand side of substance $y \in \{B_{ext}, B_{int}, A, N_{ext}, N_{int}\}$ at time t_k are.

The discretisation matrices - with the definition $dc := \frac{\Delta t}{(\Delta x)^2}$ and $fc := \frac{\Delta t v_f}{\Delta x}$ - for the substances in the biofilm have the form:

$$M_y := \begin{pmatrix} 1+dcD_y & -dcD_y & 0 & \cdots & 0 \\ -dcD_y & 1+2dcD_y & -dcD_y & \ddots & \vdots \\ 0 & \ddots & \ddots & \ddots & 0 \\ \vdots & \ddots & -dcD_y & 1+2dcD_y & -dcD_y \\ 0 & \cdots & 0 & -dcD_y & 1+dcD_y \end{pmatrix}, \text{ for } y \in \{B_{int}, A, N_{int}\}$$

The two substances in the flow have different boundary conditions and hence the discretisation matrices differ from the ones used for the substances in the biofilm as well as among themselves. The discretisation matrix for the bacteria in the flow is shown beneath.

$$M_{B_{ext}} = \begin{pmatrix} 1+dcD_{B_{ext}} & -dcD_{B_{ext}} & 0 & \cdots & 0 \\ -dcD_{B_{ext}}-fc & 1+2dcD_{B_{ext}}+fc & -dcD_{B_{ext}} & \ddots & \vdots \\ 0 & \ddots & \ddots & \ddots & 0 \\ \vdots & \ddots & -dcD_{B_{ext}}-fc & 1+2dcD_{B_{ext}}+fc & -dcD_{B_{ext}} \\ 0 & \cdots & 0 & -fc & 1+fc \end{pmatrix}$$

Last, but not least, the matrix for N_{ext} resulting from the discretisation of the time-derivative, the diffusion- and advection-term reads as follows:

$$M_{N_{ext}} := \begin{pmatrix} 1+2dcD_{N_{ext}}+fc & -dcD_{N_{ext}} & 0 & \cdots & 0 \\ -dcD_{N_{ext}}-fc & 1+2dcD_{N_{ext}}+fc & -dcD_{N_{ext}} & \ddots & \vdots \\ 0 & \ddots & \ddots & \ddots & 0 \\ \vdots & \ddots & -dcD_{N_{ext}}-fc & 1+2dcD_{N_{ext}}+fc & -dcD_{N_{ext}} \\ 0 & \cdots & 0 & -fc & 1+fc \end{pmatrix}$$

8.2 Choice of parameters

After the system has been discretised, the only missing part - before the PDE-model can be simulated - is to find suitable parameter values. Those have to be chosen carefully such that a biological relevant behaviour can be observed in the simulations.

At first, the diffusion parameters are chosen. The diffusion parameter $D_{N_{ext}}$ is obtained using the theory given in [Hob88]. Assuming the diffusion rate of nutrients within the biofilm to be one fourth of $D_{N_{ext}}$ and of AHL to be one tenth, leads to the diffusion coefficients $D_{N_{int}}$ and D_A.
As the bacteria are considerably bigger than AHL, the diffusion rates are assumed to be just a small fraction of D_A. Again, the bacteria in the biofilm are supposed to diffuse slower than the bacteria in the flow. In fact, they are assumed to be almost immobile. Those ideas lead to the diffusion constants shown in table 8.1.
The flow velocity was taken from [MMK+12]. The channel is rinsed with a nutrient-saturated fluid at $2\frac{ml}{h}$. As the flow chamber has a height of $0.4mm$ and a width of $3.8mm$, the velocity can be calculated by

$$v_f = \frac{2 \cdot 10^{12} \mu m^3/h}{400\,\mu m \cdot 3800\,\mu m}.$$

The concentration of nutrients, which is carried into the experimental set-up by the flow, was chosen arbitrarily to be 1. This is the capacity used in the ODE-model and hence a reasonable choice.
The colonisation rate c_b is chosen to be a value, which increases the simulation time only slightly, but still leads to a fast colonisation of the biofilm. It is assumed that the bacteria can sense other bacteria in the biofilm up to $250\,\mu m$ upstream and hence do not colonise the biofilm if there are bacteria present in this region.
The strength of the avoidance of recolonisation due to other bacteria, i.e., the parameter c, is arbitrarily chosen to be 1.

If not mentioned otherwise, we choose as a initial condition that the liquid within the flow chamber and biofilm is saturated with nutrients, i.e., $N_{ext0}(x) = N_{int0}(x) = 1$ for all $x \in [0, x_{end}]$. At $1mm$, $2mm$, $5mm$ and $8mm$ after the beginning of the flow chamber two bacteria are positioned in the biofilm, i.e., $B_{int0}(1000) = B_{int0}(2000) = B_{int0}(5000) = B_{int0}(8000) = 2.4 \cdot 10^{10}\, Bact/ml$. We also assume that neither bacteria in the flow nor AHL in the biofilm are present, which can be realised by rinsing the flow chamber at the beginning of an experiment.

8.3 Simulations on the PDE-model

In this part, the simulations of our model with an inhomogeneous spatial distribution are presented. A question that was raised at the beginning of this thesis, was,

Parameter	Value	Parameter	Value
c	1	c_b	$2.2 \cdot 10^4 \frac{1}{h}$
δ_b	$250\,\mu m$	$D_{B_{ext}}$	$3000\ \frac{\mu m^2}{h}$
$D_{B_{int}}$	$30\ \frac{\mu m^2}{h}$	D_A	$32325.2\ \frac{\mu m^2}{h}$
$D_{N_{ext}}$	$323252\ \frac{\mu m^2}{h}$	$D_{N_{int}}$	$80813\ \frac{\mu m^2}{h}$
n_{inflow}	1	v_f	$1.316 \cdot 10^6\ \frac{\mu m}{h}$

Table 8.1: Parameter values used in simulations. The values of the parameters used for the ODE-model are shown in table 5.1. Those will be used in the simulations of the PDE-model as well.

under which circumstances it is beneficial for the whole population to regulate the detachment of bacteria via quorum sensing in comparison to a constant detachment rate. Obviously conditions that influence this decision are the danger of being killed in the stream or the possibility of not finding enough nutrients at the new location. The parameters used in the simulations are shown in table 8.1.

Figure 8.4 shows the spatial distribution of all substances involved in our simulations after forty hours. While in the top left corner of this figure one can see, how the bacteria in the flow are distributed over the flow chamber, the distribution of the bacteria in the biofilm are shown in the middle of the upper row. Next to it the AHL-concentration is displayed. In the lower row, the nutrients in the flow are presented on the left and the nutrients in the biofilm on the right.

In figure 8.5 the density of bacteria in the biofilm as well as the AHL-concentration are displayed at different time points. While one can see B_{int} in blue, the corresponding AHL-concentration is shown in green. In the top left corner of this figure the two quantities are shown after ten hours have passed. The bacteria are still growing and the AHL-concentration is accumulating. After forty hours (seen in the middle of the top row) the initially, i.e., at the beginning of the simulation, positioned colonies have reached already its capacity, i.e., about eleven bacteria.
One can extract from this figure the sensitivity of the system to the positive feedback in the AHL-production. After forty-two hours, one sees the characteristic drop in AHL-concentration at $x \approx 4500\,\mu m$, $x \approx 7500\,\mu m$ and $x \approx 10000\,\mu m$. On the right side of this drop in AHL-concentration the threshold-density of bacteria in the biofilm, i.e., the "quorum", at which the AHL-production jump starts, has not yet been reached. A furthermore remarkable feature is the close association of the AHL-concentration with the distribution of the bacteria in the biofilm even though the diffusion of AHL is noticeably higher than the diffusion of the bacteria in the biofilm, which are almost immobile. This is due to the fact that a high rate for

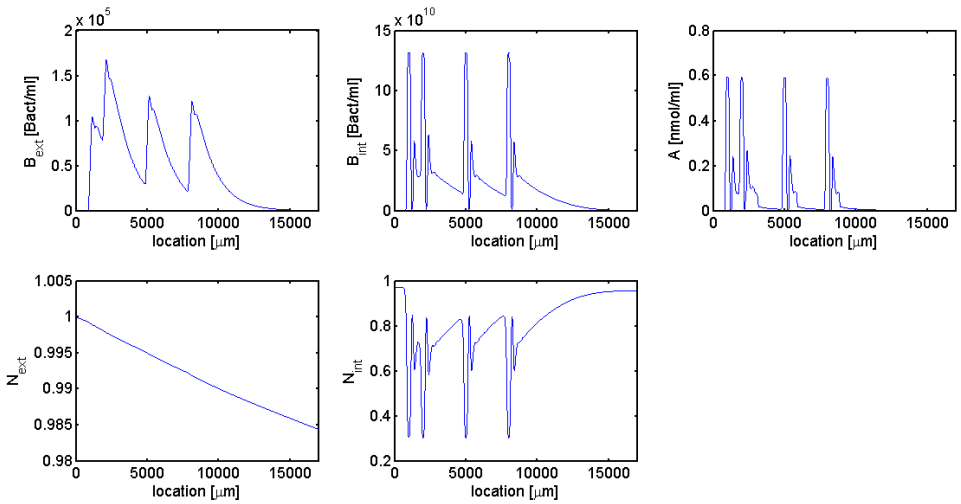

Figure 8.4: Distribution over the flow chamber of the - in our simulation - involved substances after forty hours. The death rate of the bacteria in the flow (γ_f) is $1000\frac{1}{h}$. Initially a nutrient concentration of 1 is assumed to be in the flow chamber, i.e., in the flow as well as in the biofilm. As an initial condition neither bacteria in the flow nor AHL in the biofilm are present. Two bacteria, i.e., $B_{int} = 2.4 \cdot 10^{10} Bact/ml$ are positioned at $x = 1000\,\mu m$, $x = 2000\,\mu m$, $x = 5000\,\mu m$ and $x = 8000\,\mu m$ at the beginning of the simulation. In the top left corner the density of the bacteria in the flow (B_{ext}) is shown. Middle top row: Bacterial density in the biofilm (B_{int}). Right top row: AHL-concentration in the biofilm (A). Left bottom row: Concentration of nutrients in the flow (N_{ext}). Right bottom row: Nutrient concentration in the biofilm (N_{int}).

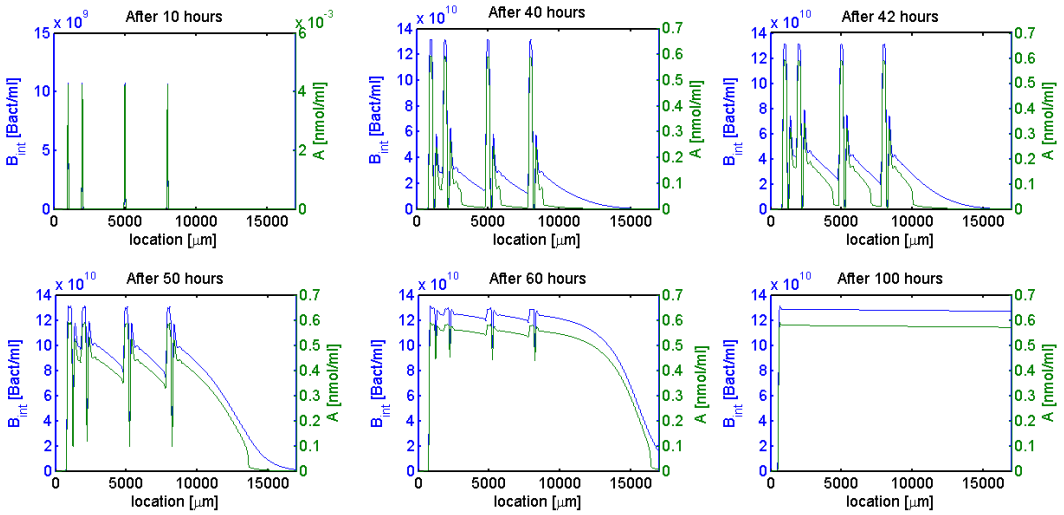

Figure 8.5: Distribution of the density of bacteria in the biofilm (blue) and of the AHL-concentration (green) in the flow chamber at different time points ($\gamma_f = 1000\,\frac{1}{h}$)

the wash out of AHL by the flow is assumed. The drop of the concentration of bacteria and AHL to the right of the initial colonies can be explained by the fact that the bacteria do not want to settle next to a place where other bacteria are already present. In the deterministic approach this effect can be only seen right next to the initial colonies. At other locations in the flow chamber this cannot be observed in our model as it is an average of the stochastic simulation, where this effect should be seen everywhere.

In figure 8.6 and 8.7 one can see the time course of the total number of bacteria. The total number is comprised of the bacteria that were washed out of the flow chamber, the bacteria in the biofilm and those in the flow. It looks as if the system does not reach a stationary phase. This is due to the wash out of the bacteria. In the flow chamber a stationary phase is reached, when the bacteria in the biofilm as well as in the flow reach its capacity. This is seen in figure 8.8. One can extract from this figure that after about 80 hours the bacteria have reached its capacity in the flow chamber everywhere but left of the first colony in the case of quorum sensing regulated detachment and the death rate of the bacteria in the flow being $1000\,\frac{1}{h}$. The simulation with those assumptions is represented by the blue line. Because of the fast flow, the bacteria need rather long to colonise the beginning of the flow chamber. The colonisation of the whole flow chamber is completed after around 150 hours. For larger death rates of the bacteria in the flow, it takes longer to reach the capacity. This is shown for $\gamma_f = 10000\,\frac{1}{h}$ in the same figure with the dashed red line. The quorum sensing regulated detachment rate averaged over the biofilm

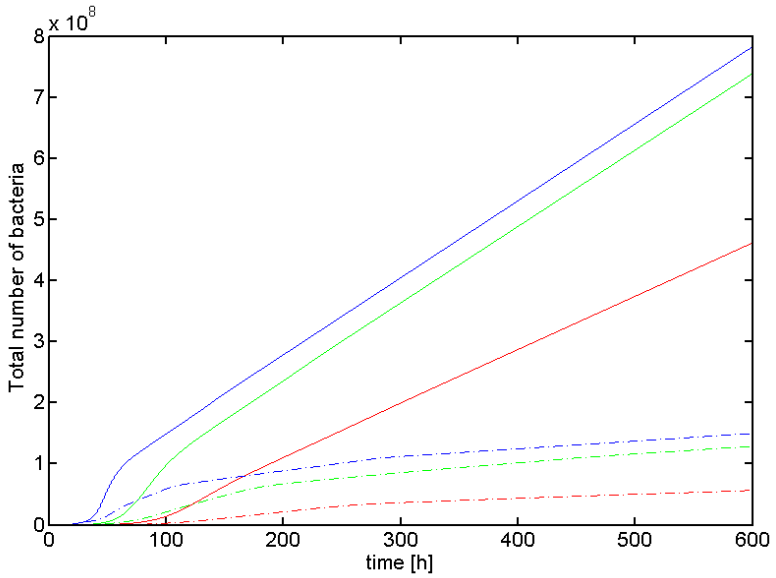

Figure 8.6: Time course of the total number of bacteria for different approaches. While the blue lines represent the quorum sensing regulated detachment, the red and green lines show the total number of bacteria for simulations with constant detachment rates. The detachment rate is $0.15\frac{1}{h}$ for the green lines and $0.2\frac{1}{h}$ for the red lines. The solid lines stand for simulations with $\gamma_f = 1000\frac{1}{h}$ and the dashed lines for $\gamma_f = 10000\frac{1}{h}$.

in the flow chamber during the course of time can be seen in figure 8.9. Again the blue line stands for a simulation with a low death rate of the bacteria in the flow ($\gamma_f = 1000\frac{1}{h}$) and the red dashed line for a high death rate ($\gamma_f = 10000\frac{1}{h}$). The correlation between the averaged detachment rate and the total number of bacteria is obvious. The detachment rate is about $0.15\frac{1}{h}$ after the stationary phase in the flow chamber is reached.

As already mentioned, the total number of bacteria in the simulation, i.e., including the bacteria washed out of the flow chamber, are displayed in figure 8.6 and 8.7 for different scenarios. In these figures the blue lines represent a quorum sensing regulated detachment, the green lines a constant detachment rate of $0.15\frac{1}{h}$ and the red lines a higher constant detachment rate of $0.2\frac{1}{h}$. While the solid lines stand for $\gamma_f = 1000\frac{1}{h}$, the dashed lines represent simulations with a death rate of the bacteria in the flow of $10000\frac{1}{h}$.

The advantage of a quorum sensing regulated detachment is obvious from these figures. While the quorum sensing regulated detachment allows the colony to grow up to a certain threshold before the detachment starts, this is not possible when a constant detachment rate is assumed. Comparing the three solid lines, i.e., small

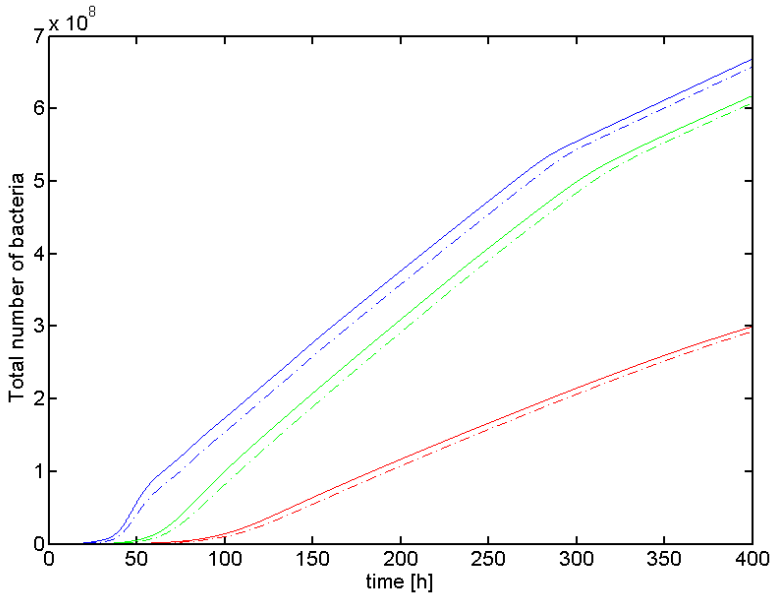

Figure 8.7: Total number of bacteria assuming a large flow chamber, i.e., the length of the flow chamber is $85mm$ instead of $17mm$. The colors were assigned to the same scenarios as in figure 8.6, i.e., quorum sensing regulated detachment in blue, low constant detachment rate ($0.15\frac{1}{h}$) in green and high detachment rate ($0.2\frac{1}{h}$) in red. Dashed lines stand for two initial colonies comprised each of two bacteria at $x = 1000\mu m$ and $x = 5000\mu m$. Solid lines additionally have two bacteria sitting at $x = 2000\mu m$ and $x = 8000\mu m$. The death rate of the bacteria in the flow is $\gamma_f = 1000\frac{1}{h}$.

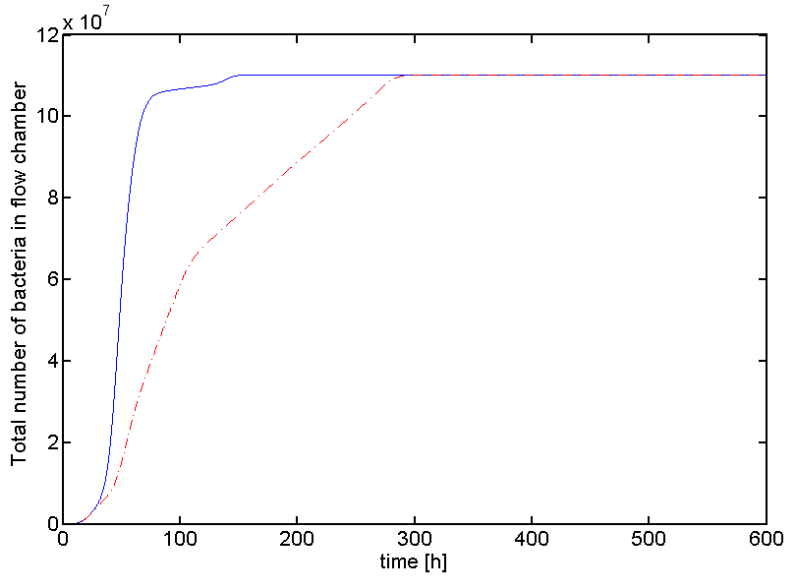

Figure 8.8: Total number of bacteria in the flow chamber, i.e., without the bacteria flowing out of the flow chamber, over the course of time. The blue line represents a simulation run with $\gamma_f = 1000\,\frac{1}{h}$ and the dashed red line shows a simulation with $\gamma_f = 10000\,\frac{1}{h}$.

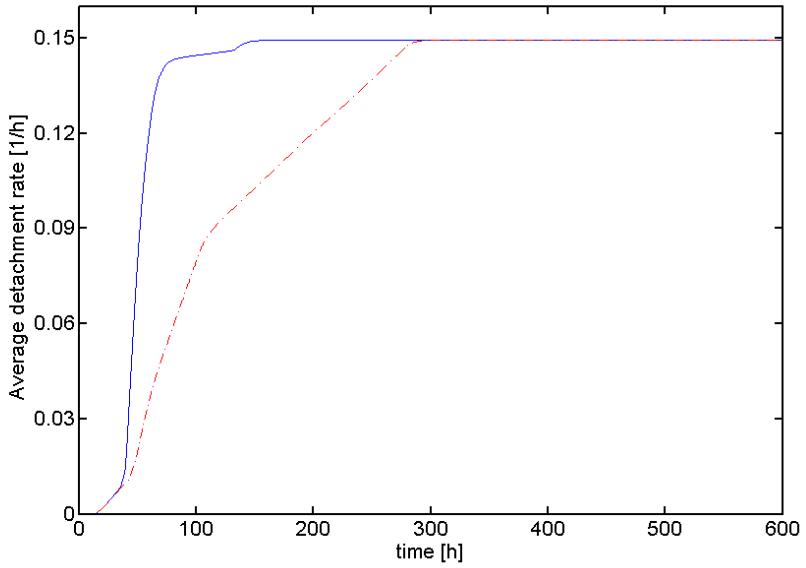

Figure 8.9: Time course of the quorum sensing regulated detachment rate averaged over the biofilm. In the simulation represented by the blue line γ_f is assumed to be $1000\,\frac{1}{h}$ and for the dashed red line γ_f is $10000\,\frac{1}{h}$.

death rate of the bacteria in the flow, among each other, shows that the bacteria in the AHL-regulated detachment have an advantage especially in the beginning of the simulation. This is not surprising, when one refers to figure 8.9, where the average detachment rate can be seen. Just after about 80 hours, the average detachment rate is at the same level as it is in the simulation represented by the green line. The advantage is kept over the whole simulation, resulting in a higher total number of bacteria for the quorum sensing regulated detachment. The simulation with the higher detachment rate (red line) obviously has an even bigger disadvantage, therefore showing a considerably lower amount of bacteria. Comparing the solid lines with the dashed lines in figure 8.6, one observes, especially in the case of the blue lines that in the beginning of the simulation the growth of the bacteria is approximately the same. This is due to the growth of the - already at the beginning of the simulation positioned - colonies. But when it comes to the recolonisation of the biofilm with detached bacteria, the two lines split and finally the simulation with the lower death rate in the flow exhibits a considerably higher number of bacteria at the end than the simulation with $\gamma_f = 10000\,\frac{1}{h}$.

The total number of bacteria at the end of the different simulations of figure 8.6 can be used to calculate ratios between the different scenarios, i.e., constant detachment rates and the AHL-regulated detachment. In the case of $\gamma_f = 1000\,\frac{1}{h}$ this is 0.944 for the ratio between the simulation with a detachment rate of $0.15\,\frac{1}{h}$ and the AHL-regulated detachment and 0.590 for the ratio between the approach with a detachment rate of $0.2\,\frac{1}{h}$ and the AHL-regulated detachment. These ratios decrease to 0.860 and 0.379 for $\gamma_f = 10000\,\frac{1}{h}$. Therefore, the advantage of the bacteria using a quorum sensing regulated detachment compared to bacteria using constant detachment rates increases with increasing death rates γ_f. This increase is greater for high detachment rates ($0.20\,\frac{1}{h}$) in comparison to small detachment rates ($0.15\,\frac{1}{h}$).

In figure 8.7 the colors are assigned to the same scenarios as in figure 8.6, i.e., the different detachment mechanisms. The death rate of the bacteria in the flow is $1000\,\frac{1}{h}$ in this figure. While the dashed lines stand for two bacteria at $x = 1000\,\mu m$ and $x = 5000\,\mu m$ at the beginning of the simulation, the solid lines represent the same initial conditions as seen in the other simulations, i.e. additionally at $x = 2000\,\mu m$ and $x = 8000\,\mu m$ two bacteria are situated. The flow chamber is assumed to be larger here than in the simulations before, i.e., $85\,mm$ instead of $17\,mm$ long. One can see that there is only a slight difference between the scenario with two starting colonies and the scenario with four starting colonies.

In this case the advantage of bacteria using quorum sensing regulated detachment compared to bacteria using constant detachment rates is even more obvious at the beginning of the simulation than in the case of a small flow chamber. This is not surprising as many bacteria die in this long flow chamber, which therefore favors mechanisms, where the bacteria stay in the biofilm. Again using the ratios at the end of the simulation, i.e., after 400 hours in this case, shows about the same value

for the ratio between detachment rate of $0.15\,\frac{1}{h}$ and AHL-regulated detachment, but with 0.448 a slightly smaller value for the ratio between $0.2\,\frac{1}{h}$ and the AHL-regulated detachment.

9 Summary and Outlook

A motivation of this thesis was the mathematical modelling of a biological experiment similar to the one found in [MMK$^+$12].

In a first step, we modelled this set-up assuming a homogeneous distribution of all occuring substances. The model was then analysed for positivity to make sure that it permits us to explain the biology of the experiment. The spatially homogeneous model was used to find values for the parameters, which have not yet been discussed in the literature, by choosing the values in the simulations in such a fashion that a reasonable behaviour of the system could be observed. In the simulations we were also able to find a Hopf bifurcation for a certain range of parameters in our system. Interestingly, an oscillating biofilm thickness has been found already in other biological experiments. Even though the density of bacteria in the biofilm was rather small in the deterministic approach, it is most likely to find such an oscillating behaviour *in vitro* as well.

In the second part of this thesis, we additionally took a spatial distribution of the occurring substances into account. The new model was then analysed for positivity again to validate it for the purpose of explaining the biological experiment. Afterwards, we adapted the model slightly such that we could concentrate on a possible pattern formation during no-flow conditions. No proof of a pattern formation could be found. This is due to the fact that the non-trivial stationary state is stable for all wave-numbers k^2 as it was shown in our analysis. Therefore, all spatial variations under no-flow conditions vanish after a long period of time and hence waiting long enough leads to a spatially homogeneous distribution of the substances in the biofilm.

Last, but not least, simulations of the flow chamber model were carried out. We found that bacteria using a quorum sensing regulated detachment mechanism increase their numbers in the beginning of the simulations faster than bacteria having constant detachment rates. On the one hand in the long-term behaviour of the simulation the increase of the size of the flow chamber has no effect on the ratio between the total number of bacteria using AHL-regulated detachment and bacteria having a comparable constant detachment rate ($0.15\,\frac{1}{h}$). On the other hand the advantage of the quorum sensing regulated detachment compared to a constant detachment rate is greater in large flow chambers than in small ones at the early stages of the simulation. Starting with two or four colonies does not favour any of the two

approaches. The death rate of the bacteria in the flow has a great influence on the decision of which approach - quorum sensing regulated or constant detachment - is better for the whole population. The higher the death rate is, the more likely is it that quorum sensing regulated detachment is favourable for the whole population compared to the constant detachment of bacteria from the biofilm.

Further work in this field could include the use of discrete values to account for the number of bacteria instead of bacterial densities. This would solve the problem of partial bacteria as it was seen in our approach. Using this, the reproduction and recolonisation should be changed as well. They should be modelled using Poisson processes. This would lead to more accurate results as this allows for separate colonies to form. It is not possible to see a formation of separate colonies in our biological set-up, when a model comprised of partial differential equations without stochasticity - as in this thesis - is used. Another possible extension would be the influence of nutrients on the production of AHL as described in [KKCH13]. One could also consider the effect of lactonase on the degradation of AHL. This relation has been postulated to some extent in [FKR$^+$10]. Last, but not least, the negative effect of the AHL-production - as it is energy consuming - on the reproduction of the bacteria could be included.

A Pattern formation

A.1 Derivation of the stability conditions shown in section 7.2.2 and in 7.2.3

Let $f_i, g_i, h_i \in \mathbb{R}\ \forall i \in \{1,2,3\}$ and assume the following form of the Jacobian and the Diffusion matrix:

$$L := \begin{pmatrix} f_1 & f_2 & f_3 \\ g_1 & g_2 & g_3 \\ h_1 & h_2 & h_3 \end{pmatrix} \quad \text{and} \quad D := \begin{pmatrix} D_1 & 0 & 0 \\ 0 & D_2 & 0 \\ 0 & 0 & D_3 \end{pmatrix} \tag{A.1}$$

Hence, we need the characteristic equation to calculate the eigenvalues of L:

$$\det(\lambda I - L) = 0$$

This leads to the characteristic polynomial:

$$\lambda^3 - \underbrace{(f_1 + g_2 + h_3)}_{=\mathrm{tr}(L)\widehat{=}a_1}\lambda^2 + \underbrace{(f_1g_2 - g_1f_2 + f_1h_3 - f_3h_1 + g_2h_3 - g_3h_2)}_{=:\mathrm{r}(L)\widehat{=}a_2}\lambda - \underbrace{(f_1g_2h_3 - f_1g_3h_2 - g_1f_2h_3 + g_1f_3h_2 + h_1f_2g_3 - h_1f_3g_2)}_{=\det(L)\widehat{=}a_3} = 0$$

Thereby one arrives at the conditions shown in (7.16) in section 7.2.2 when applying the Routh-Hurwitz stability criterion.
Introducing diffusion yields:

$$\det(L - k^2D - \lambda I) = 0$$

Expansion of this equation leads to:

$$\begin{aligned}
&\lambda^3 + \lambda^2\left[(D_1 + D_2 + D_3)k^2 - (f_1 + g_2 + h_3)\right] + \\
&\lambda\left[(f_1g_2 - g_1f_2 + f_1h_3 - h_1f_3 + g_2h_3 - g_3h_2) + (D_1D_2 + D_1D_3 + D_2D_3)k^4\right. \\
&\quad \left. - (f_1(D_2 + D_3) + g_2(D_1 + D_3) + h_3(D_1 + D_2))k^2\right] \\
&+ [D_1D_2D_3k^6 - (f_1D_2D_3 + g_2D_1D_3 + h_3D_1D_2)k^4 \\
&+ (D_1(g_2h_3 - g_3h_2) + D_2(f_1h_3 - f_3h_1) + D_3(f_1g_2 - f_2g_1))\,k^2 \\
&- (f_1g_2h_3 - f_1g_3h_2 - g_1f_2h_3 + g_1f_3h_2 + h_1f_2g_3 - h_1f_3g_2)] = 0
\end{aligned}$$

This explains the form of condition (7.22) in section 7.2.3.

A.2 Outline for Turing pattern formation

Outline for conditions to observe a Turing pattern in a three-dimensional system:

1. Stationary state of spatially homogeneous model is stable, i.e., $Re(\lambda_i(k^2 = 0)) < 0 \; \forall i \in \{1, 2, 3\}$.

2. Stationary state is unstable when introducing diffusion, i.e., $\exists \; k^2 > 0, \exists \; i \in \{1, 2, 3\} : Re(\lambda_i(k^2)) > 0$.
   This is true, if the following conditions are fulfilled:

   a) $a_1 > 0$

   b) $a_2 > 0$

   c) $a_3 = P(k^2)$ switches sign for positive k^2, i.e.,

      i. $\frac{dP(k_c^2)}{dk^2} = 0$

      ii. $k_c^2 > 0 \Leftrightarrow \begin{cases} b_1^2 - 3b_0b_2 > 0 \\ b_1 > 0 \text{ or } b_2 < 0 \end{cases}$

      iii. $P(k_c^2) < 0$

If the above conditions in a three-dimensional model are fulfilled, one can observe the formation of a Turing pattern in this system.

A.3 Polynomial used in wave-instability pattern formation

Using the definitions of L and D found in equation (A.1) yields:

$$\begin{aligned} P_1(k^2) :=& a_1a_2 - a_3 = \\ & \big(k^2(D_1 + D_2 + D_3) - \mathrm{tr}(L)\big) \cdot \\ & \cdot \big(\mathrm{r}(L) + k^4(D_1D_2 + D_1D_3 + D_2D_3) - k^2(f_1(D_2 + D_3) + g_2(D_1 + D_3) + h_3(D_1 + D_2))\big) \\ & - P(k^2) = ak^6 + bk^4 + ck^2 + d, \end{aligned}$$

with

$$
\begin{aligned}
a =& D_1^2(D_2+D_3)+D_2^2(D_1+D_3)+D_3^2(D_1+D_2)+2D_1D_2D_3\\
b =& -2\left(f_1(D_2^2+D_3^2)+g_2(D_1^2+D_3^2)+h_3(D_1^2+D_2^2)+2(f_1+g_2+h_3)(D_1D_2+D_1D_3+D_2D_3)\right)\\
c =& 2(f_1g_2+f_1h_3+g_2h_3)(D_1+D_2+D_3)+f_1^2(D_2+D_3)+g_2^2(D_1+D_3)+h_3^2(D_1+D_2)\\
& -f_2g_1(D_1+D_2)-f_3h_1(D_1+D_3)-g_3h_2(D_2+D_3)\\
d =& -f_1^2(g_2+h_3)-g_2^2(f_1+h_3)-h_3^2(f_1+g_2)-2f_1g_2h_3+f_3g_1h_2+f_2g_3h_1+f_1f_2g_1+f_1f_3h_1\\
& +f_2g_1g_2+g_2g_3h_2+f_3h_1h_3+g_3h_2h_3
\end{aligned}
$$

A.4 Outline for pattern formation due to a wave-instability

Outline for conditions to observe a pattern due to a wave-instability in a three-dimensional system:

1. Stationary state of spatially homogeneous model is stable, i.e., $Re(\lambda_i(k^2 = 0)) < 0 \ \forall i \in \{1,2,3\}$.

2. Stationary state is unstable when introducing diffusion, i.e., $\exists\ k^2 > 0, \exists\ i \in \{1,2,3\} : Re(\lambda_i(k^2)) > 0$.
   This is true, if the following conditions are fulfilled:
   a) $a_1 > 0$
   b) $a_2 > 0$
   c) $a_3 > 0$
   d) $a_1a_2 - a_3 = P_1(k^2)$ switches sign for positive k^2, i.e.,
      i. $\frac{dP_1(k_c^2)}{dk^2} = 0$
      ii. $k_c^2 > 0 \Leftrightarrow \begin{cases} b^2 - 3ac > 0 \\ b > 0 \text{ or } c < 0 \end{cases}$
      iii. $P(k_c^2) < 0$

If the above conditions in a three-dimensional model are fulfilled, one can observe the formation of a pattern due to a wave-instability in this system.

B Discretisation

B.1 Central difference scheme

Adding the equations of the *backward difference scheme* to the equation of the *forward difference scheme* leads - for the approximation of the first derivative with respect to space - to:

$$\frac{u_{j+1} - u_{j-1}}{2\Delta x} = \frac{\partial u(x_j)}{\partial x} + O((\Delta x)^2) \tag{B.1}$$

B.2 Discretised model

In this part of the appendix, the whole model is listed in its discretised form. First of all, the discretised governing equations in the inner domain are shown. Afterwards, the equations at the spatial boundaries of the substances in the biofilm are presented. At last, the equations at the spatial boundaries of the bacteria and nutrients in the flow are written down.

The discretisation of the governing equations of model (6.3) without boundaries, i.e., for all $j \in \{1, \dots, Nx-2\}$ and $k \in \{1, \dots, Nt-1\}$:

$$\begin{aligned} B_{ext,j}^{k+1} - \frac{\Delta t}{(\Delta x)^2} D_{B_{ext}} \left(B_{ext,j+1}^{k+1} - 2B_{ext,j}^{k+1} + B_{ext,j-1}^{k+1} \right) + \frac{\Delta t}{\Delta x} v_f \left(B_{ext,j}^{k+1} - B_{ext,j-1}^{k+1} \right) = \\ = B_{ext,j}^{k} + \Delta t \left(-\frac{c_b}{\eta} \operatorname{col}(B_{int,j}^{k}) B_{ext,j}^{k} + \frac{c_A}{\eta} B_{int,j}^{k} \frac{A_j^k}{A_{thr1} + A_j^k} - \gamma_f B_{ext,j}^{k} \right) \end{aligned}$$

$$\begin{aligned} B_{int,j}^{k+1} - \frac{\Delta t}{(\Delta x)^2} D_{B_{int}} \left(B_{int,j+1}^{k+1} - 2B_{int,j}^{k+1} + B_{int,j-1}^{k+1} \right) = \\ = B_{int,j}^{k} + \Delta t \left(c_b \operatorname{col}(B_{int,j}^{k}) B_{ext,j}^{k} - c_A B_{int,j}^{k} \frac{A_j^k}{A_{thr1} + A_j^k} + \beta_{int} B_{int,j}^{k} \frac{N_{int,j}^{k}}{N_{thr} + N_{int,j}^{k}} \right) \end{aligned}$$

$$A_j^{k+1} - \frac{\Delta t}{(\Delta x)^2} D_A \left(A_{j+1}^{k+1} - 2A_j^{k+1} + A_{j-1}^{k+1} \right) = \\ = A_j^k \Delta t \left(B_{int,j}^k (\alpha_A + \beta_A \frac{(A_j^k)^2}{A_{thr2}^2 + (A_j^k)^2}) - (\gamma_A + d_v) A_j^k \right)$$

$$N_{ext,j}^{k+1} - \frac{\Delta t}{(\Delta x)^2} D_{N_{ext}} \left(N_{ext,j+1}^{k+1} - 2N_{ext,j}^{k+1} + N_{ext,j-1}^{k+1} \right) + \frac{\Delta t}{\Delta x} v_f \left(N_{ext,j}^{k+1} - N_{ext,j-1}^{k+1} \right) = \\ = N_{ext,j}^k + \Delta t \left(-\frac{c_N}{\eta} (N_{ext,j}^k - N_{int,j}^k) - \gamma_N N_{ext,j}^k \right)$$

$$N_{int,j}^{k+1} - \frac{\Delta t}{(\Delta x)^2} D_{N_{int}} \left(N_{int,j+1}^{k+1} - 2N_{int,j}^{k+1} + N_{int,j-1}^{k+1} \right) = \\ = N_{int,j}^k + \Delta t \left(c_N (N_{ext,j}^k - N_{int,j}^k) - c_1 B_{int,j}^k \frac{N_{int,j}^k}{N_{thr} + N_{int,j}^k} - \gamma_N N_{int,j}^k \right)$$

Discretisation on the left boundary of the substances in the biofilm, i.e., $j = 0$ and $k \in \{1, \ldots, Nt - 1\}$:

$$B_{int,0}^{k+1} - \frac{\Delta t}{(\Delta x)^2} D_{B_{int}} \left(B_{int,1}^{k+1} - B_{int,0}^{k+1} \right) = \\ = B_{int,0}^k + \Delta t \left(c_b \, \mathrm{col}(B_{int,0}^k) B_{ext,0}^k - c_A B_{int,0}^k \frac{A_0^k}{A_{thr1} + A_0^k} + \beta_{int} B_{int,0}^k \frac{N_{int,0}^k}{N_{thr} + N_{int,0}^k} \right)$$

$$A_0^{k+1} - \frac{\Delta t}{(\Delta x)^2} D_A \left(A_1^{k+1} - A_0^{k+1} \right) = \\ = A_0^k \Delta t \left(B_{int,0}^k (\alpha_A + \beta_A \frac{(A_0^k)^2}{A_{thr2}^2 + (A_0^k)^2}) - (\gamma_A + d_v) A_0^k \right)$$

$$N_{int,0}^{k+1} - \frac{\Delta t}{(\Delta x)^2} D_{N_{int}} \left(N_{int,1}^{k+1} - N_{int,0}^{k+1} \right) = \\ = N_{int,0}^k + \Delta t \left(c_N (N_{ext,0}^k - N_{int,0}^k) - c_1 B_{int,0}^k \frac{N_{int,0}^k}{N_{thr} + N_{int,0}^k} - \gamma_N N_{int,0}^k \right)$$

Right boundary for substances in the biofilm, i.e., $j = Nx-1$ and $k \in \{1, \ldots, Nt-1\}$:

$$B^{k+1}_{int,Nx-1} - \frac{\Delta t}{(\Delta x)^2} D_{B_{int}} \left(B^{k+1}_{int,Nx-2} - B^{k+1}_{int,Nx-1} \right) =$$
$$= B^{k}_{int,Nx-1} + \Delta t \left(c_b \, \mathrm{col}(B^{k}_{int,Nx-1}) B^{k}_{ext,Nx-1} - c_A B^{k}_{int,Nx-1} \frac{A^{k}_{Nx-1}}{A_{thr1} + A^{k}_{Nx-1}} \right.$$
$$\left. + \beta_{int} B^{k}_{int,Nx-1} \frac{N^{k}_{int,Nx-1}}{N_{thr} + N^{k}_{int,Nx-1}} \right)$$

$$A^{k+1}_{Nx-1} - \frac{\Delta t}{(\Delta x)^2} D_A \left(A^{k+1}_{Nx-2} - A^{k+1}_{Nx-1} \right) =$$
$$= A^{k}_{Nx-1} + \Delta t \left(B^{k}_{int,Nx-1} (\alpha_A + \beta_A \frac{(A^{k}_{Nx-1})^2}{A^2_{thr2} + (A^{k}_{Nx-1})^2}) - (\gamma_A + d_v) A^{k}_{Nx-1} \right)$$

$$N^{k+1}_{int,Nx-1} - \frac{\Delta t}{(\Delta x)^2} D_{N_{int}} \left(N^{k+1}_{int,Nx-2} - N^{k+1}_{int,Nx-1} \right) =$$
$$= N^{k}_{int,Nx-1} + \Delta t \left(c_N (N^{k}_{ext,Nx-1} - N^{k}_{int,Nx-1}) - c_1 B^{k}_{int,Nx-1} \frac{N^{k}_{int,Nx-1}}{N_{thr} + N^{k}_{int,Nx-1}} - \gamma_N N^{k}_{int,Nx-1} \right)$$

Left boundaries for substances in the flow:

$$B^{k+1}_{ext,0} - \frac{\Delta t}{(\Delta x)^2} D_{B_{ext}} \left(B^{k+1}_{ext,1} - B^{k+1}_{ext,0} \right) =$$
$$= B^{k}_{ext,0} + \Delta t \left(-\frac{c_b}{\eta} \, \mathrm{col}(B^{k}_{int,0}) B^{k}_{ext,0} + \frac{c_A}{\eta} B^{k}_{int,0} \frac{A^{k}_{0}}{A_{thr1} + A^{k}_{0}} - \gamma_f B^{k}_{ext,0} \right)$$

$$N^{k+1}_{ext,0} - \frac{\Delta t}{(\Delta x)^2} D_{N_{ext}} \left(N^{k+1}_{ext,1} - 2N^{k+1}_{ext,0} \right) + \frac{\Delta t}{\Delta x} v_f N^{k+1}_{ext,0} =$$
$$= N^{k}_{ext,0} + \Delta t \left(-\frac{c_N}{\eta} \left(N^{k}_{ext,0} - N^{k}_{int,0} \right) - \gamma_N N^{k}_{ext,0} \right) + \left(\frac{\Delta t}{(\Delta x)^2} D_{N_{ext}} + \frac{\Delta t}{\Delta x} v_f \right) n_{inflow}$$

Right boundaries for substances in the flow:

$$
\begin{aligned}
&B^{k+1}_{ext,Nx-1} + \frac{\Delta t}{\Delta x} v_f \left(B^{k+1}_{ext,Nx-1} - B^{k+1}_{ext,Nx-2} \right) = \\
=&B^{k}_{ext,Nx-1} + \\
&+ \Delta t \left(-\frac{c_b}{\eta} \operatorname{col}(B^k_{int,Nx-1}) B^k_{ext,Nx-1} + \frac{c_A}{\eta} B^k_{int,Nx-1} \frac{A^k_{Nx-1}}{A_{thr1} + A^k_{Nx-1}} - \gamma_f B^k_{ext,Nx-1} \right)
\end{aligned}
$$

$$
\begin{aligned}
N^{k+1}_{ext,Nx-1} + \frac{\Delta t}{\Delta x} v_f \left(N^{k+1}_{ext,Nx-1} - N^{k+1}_{ext,Nx-2} \right) = \\
= N^k_{ext,Nx-1} + \Delta t \left(-\frac{c_N}{\eta} \left(N^k_{ext,Nx-1} - N^k_{int,Nx-1} \right) - \gamma_N N^k_{ext,Nx-1} \right)
\end{aligned}
$$

Bibliography

[Bra11] V. Brandstetter. Analysis of reaction-diffusion models for bacterial cell-cell communication. Diploma thesis, Dept. of Mathematics, Technische Universität München, Germany, 2011.

[CLC+95] W.J. Costerton, Z. Lewandowski, D.E. Caldwell, D.R. Korber, and H.M. Lappin-Scott. Microbial Biofilms. *Annu. Rev. Microbiol.*, 49:711–745, 1995.

[DK01] J. Dockery and J. Keener. A mathematical model for quorum sensing in *Pseudomonas aeruginosa*. *Bull. Math. Biol.*, 63:95–116, 2001.

[DZRE00] M. Dolnik, A.M. Zhabotinsky, A.B. Rovinsky, and I.R. Epstein. Spatio-temporal patterns in a reaction-diffusion system with wave instability. *Chem. Eng. Sci.*, 55:223–231, 2000.

[EK05] L. Edelstein-Keshet. *Mathematical Models in Biology*. SIAM, Philadelphia, 2005.

[Eng94] R. Engelhardt. Modelling pattern formation in reaction-diffusion systems. Master's thesis, Dept. of Chemistry, University of Copenhagen, Denmark, 1994.

[Erm03] B. Ermentrout. XPPAUT Version 5.41. `http://www.math.pitt.edu/~bard/bardware/`, February 2003.

[ES10] M.A. Efendiev and S. Sonner. On verifying mathematical models with diffusion, transport and interaction. *Advances in Math. Sci. Appls*, 32:41–67, 2010.

[Eva10] L.C. Evans. *Partial Differential Equations*. American Mathematical Society, Providence, Rhode Island, 2010.

[Fis03] G. Fischer. *Lineare Algebra*. Friedr. Vieweg & Sohn Verlag, Wiesbaden, 2003.

[FKR+10] A. Fekete, C. Kuttler, M. Rothballer, B.A. Hense, D. Fischer, K. Buddrus-Schiemann, M. Lucio, J. Müller, P. Schmitt-Kopplin, and A. Hartmann. Dynamic Regulation of N-Acyl-homoserine Lactone Production and Degradation in *Pseudomonas putida* IsoF. *FEMS Microbiol. Ecol.*, 72:22–34, 2010.

[GH02] J. Guckenheimer and P. Holmes. *Nonlinear Oscillations, Dynamical Systems and Bifurcations of Vector Fields*. Springer-Verlag, New York, 2002.

[Gri96] P. Grindrod. *The Theory and Applications of Reaction-Diffusion Equations: Patterns and Waves*. Oxford University Press, New York, 1996.

[Hen81] D. Henry. *Geometric Theory of Semilinear Parabolic Equations*. Springer-Verlag, Berlin, 1981.

[HKM+07] B.A. Hense, C. Kuttler, J. Müller, M. Rothballer, A. Hartmann, and J. Kreft. Does efficiency sensing unify diffusion and quorum sensing? *Nat. Rev. Microbiol.*, 5:230–239, 2007.

[HNA13] S. Hata, H. Nakao, and Mikhailov A.S. Sufficient conditions for wave instability in three-component reaction-diffusion systems. *arXiv*, page 1302.0683v2, 2013.

[Hob88] R. Hobbie. *Intermediate physics for medicine and biology*. Wiley, London, 1988.

[HV03] W. Hundsdorfer and J.G. Verwer. *Numerical Solution of Time-Dependent Advection-Diffusion-Reaction Equations*. Springer-Verlag, Berlin, 2003.

[KH08] C. Kuttler and B.A. Hense. Interplay of two quorum sensing regulation systems of *Vibrio fischeri*. *J. Theor. Biol.*, 251:167–180, 2008.

[KKCH13] P. Kumberger, C. Kuttler, P. Czuppon, and B.A. Hense. Multiple regulation mechanisms of bacterial quorum sensing, 2013. in preparation.

[Kut09] C. Kuttler. Mathematical models in biology. Lecture Notes, Technische Universität München, 2009.

[Kuz04] Y.A. Kuznetsov. *Elements of Applied Bifurcation Theory*. Springer-Verlag, New York, 2004.

[Mat10] The MathWorks. MATLAB Version R2010a. `http://www.mathworks.de/`, March 2010.

[MMK+12] A. Meyer, J.A. Megerle, C. Kuttler, J. Müller, C. Aguilar, L. Eberl, B.A. Hense, and J.O. Rädler. Dynamics of AHL mediated quorum sensing under flow and non-flow conditions. *Phys. Biol.*, 9:026007, 2012.

[Mur02] J.D. Murray. *Mathematical Biology I: An Introduction*. Springer-Verlag, Berlin, 2002.

[Mur03] J.D. Murray. *Mathematical Biology II: Spatial Models and Biomedical Applications*. Springer-Verlag, Berlin, 2003.

[PF10] T.G. Platt and C. Fuqua. What's in a name? The semantics of quorum sensing. *Trends Microbiol.*, 18:383–387, 2010.

[Pie77] E.C. Pielou. *Mathematical Ecology*. John Wiley & Sons, New York, 1977.

[PSL97] F. Padilla, Y. Secretan, and M. Leclerc. On open boundaries in the finite element approximation of two-dimensional advection-diffusion flows. *Int. J. Num. Meth. Eng.*, 40:2493–2516, 1997.

[Red02] R.J. Redfield. Is quorum sensing a side effect of diffusion sensing? *Trends Microbiol.*, 10:365–370, 2002.

[Tur52] A.M. Turing. The chemical basis of morphogenesis. *Phil. Trans. Roy. Soc. of London, Series B: Biological Sciences*, 237:37–72, 1952.

[Wer11] D. Werner. *Funktionalanalysis*. Springer-Verlag, Berlin, 2011.

[ZDE95] A.M. Zhabotinsky, M. Dolnik, and I.R. Epstein. Pattern formation arising from wave instability in a simple reaction-diffusion system. *J. of Chem. Phys.*, 103:10306–10314, 1995.

[ZKR+99] W. Ziebuhr, V. Krimmer, S. Rachid, I. Lößner, F. Götz, and J. Hacker. A novel mechanism of phase variation of virulence in *Staphylococcus epidermidis*: evidence for control of the polysaccharide intercellular adhesin synthesis by alternating insertion and excision of the insertion sequence element IS*256*. *Mol. Microbiol.*, 32:345–356, 1999.

List of Figures

List of Tables